



eCOMMONS

Loyola University Chicago
Loyola eCommons

Master's Theses

Theses and Dissertations

1997

The Application of Matrix Assisted Laser Desorption Ionization Time of-Flight Mass Spectrometry (Maldi ToF Ms) for DNA Adducts and Cross-Linked Hemoglobin Analysis

Xiaomei Gu

Follow this and additional works at: https://ecommons.luc.edu/luc_theses

 Part of the [Chemistry Commons](#)

This Thesis is brought to you for free and open access by the Theses and Dissertations at Loyola eCommons. It has been accepted for inclusion in Master's Theses by an authorized administrator of Loyola eCommons. For more information, please contact ecommons@luc.edu.



This work is licensed under a [Creative Commons Attribution-NonCommercial-No Derivative Works 3.0 License](#).
Copyright © 1997 Xiaomei Gu

LOYOLA UNIVERSITY OF CHICAGO

THE APPLICATION OF MATRIX ASSISTED LASER DESORPTION
IONIZATION TIME-OF-FLIGHT MASS SPECTROMETRY
(MALDI TOF MS) FOR DNA ADDUCTS AND CROSS-
LINKED HEMOGLOBIN ANALYSIS

A THESIS SUBMITTED TO THE FACULTY OF THE GRADUATE SCHOOL
IN CANDIDACY FOR THE DEGREE OF MASTER OF SCIENCE

DEPARTMENT OF CHEMISTRY

BY

XIAOMEI GU

CHICAGO, ILLINOIS

JANUARY, 1997

**Copyright by Xiaomei Gu, 1997
All right Reserved**

TABLE OF CONTENTS

LIST OF FIGURES.....	v
LIST OF SCHEMES.....	viii
LIST OF ABBREVIATION.....	ix
LIST OF TABLES.....	ix

CHAPTER

I INTRODUCTION.....	1
Development of matrix-assisted laser desorption ionization.....	6
Matrix.....	7
Instrumentation.....	9
Appilcations: Protein analysis.....	14
Problem Statement.....	22
II EXPERIMENTAL SECTION.....	24
Materials and methods.....	24

Synthesis of matrices	26
Preparation for identifying cross-linked hemoglobin sites.....	27
MALDI-TOF MS	32
III MATRICES SYNTHESIZING AND EVALUATION	37
Synthesis of matrices	38
Matrix evaluation	51
IV IDENTIFYING CROSS-LINKED HEMOGLOBIN BINDING SITES	67
Identifying α 99XLHb and β 82XLHb cross-linked site	
by trypsin digestion	71
MALDI mass mapping of cross-linked hemoglobinwith cyanogen	
bromide digestion	81
Identifying unknown cross-linked hemoglobin	91
REFERENCES	95
VITA	102

LIST OF FIGURES

Fig. 1.	Electrospray mass spectrometry source	3
Fig. 2.	MALDI mass spectrometry source	4
Fig. 3.	Diagram of linear mode time-of-flight.....	12
Fig. 4.	Diagram of reflectron mode time-of-flight.....	13
Fig. 5.	MALDI MS spectrum of cytochrome C with 4HCC as matrix	16
Fig. 6.	MALDI MS spectrum of 4-hydroxy- α -cyanocinnamic acid.....	17
Fig. 7.	Scheme of MALDI-TOF instrument used in experiment	34
Fig. 8.	NMR spectrum of 4-benzyloxy- α -cyanocinnamic acid	41
Fig. 9.	IR spectrum of 4-benzyloxy- α -cyanocinnamic acid.....	42
Fig. 10.	UV spectrum of 4-benzyloxy- α -cyanocinnamic acid.....	43
Fig. 11.	MALDI MS spectrum of 4-benzyloxy- α -cyanocinnamic acid	44
Fig. 12.	NMR spectrum of 4-phenyl- α -cyanocinnamic acid	47
Fig. 13.	IR spectrum of 4-phenyl- α -cyanocinnamic acid	48
Fig. 14.	UV spectrum of 4-phenyl- α -cyanocinnamic acid.....	49

Fig. 15.	MALDI MS spectrum of 4-phenyl- α -cyanocinnamic acid	50
Fig. 16A.	MALDI MS spectrum of 2'-deoxyguanosine with 4HCC as matrix	53
Fig. 16B.	MALDI MS spectrum of 2'-deoxyguanosine with BCC as matrix	54
Fig. 16C.	MALDI MS spectrum of 2'-deoxyguanosine with PCC as matrix.....	55
Fig. 17A.	MALDI MS spectrum of dGC8AAF with 4HCC as matrix	59
Fig. 17B.	MALDI MS spectrum of dGC8AAF with PCC as matrix.....	60
Fig. 18.	MALDI MS spectra of bovine insulin in (A) BCC and (B) PCC matrices.....	63
Fig. 19.	MALDI MS spectra of bovine insulin in (A) CA and (B) FA matrices	64
Fig. 20.	MALDI MS spectra of bovine insulin in (A) SA and (B) DHB matrices.....	65
Fig. 21.	MALDI MS spectrum of bovine insulin in a 4HCC matrix.....	66
Fig. 22.	MALDI MS of tryptic digest of hemoglobin.....	73
Fig. 23.	MALDI MS spectrum of tryptic digest of α 99XLHb.....	78
Fig. 24.	MALDI MS spectrum of tryptic digest of β 82XLHb	79
Fig. 25.	MALDI MS spectrum of tryptic digest of α 99XLHb	80
Fig. 26.	MALDI MS spectrum of CNBr digest of α 99XLHb.....	84

Fig. 27.	MALDI MS spectrum of CNBr digest of β 82XLHb	85
Fig. 28.	MALDI MS spectrum of CNBr digest of hemoglobin.....	86
Fig. 29.	MALDI MS spectrum of tryptic digest of α 99XLHb CNBr fragment.....	89
Fig. 30.	MALDI MS spectrum of tryptic digest of β 82XLHb CNBr fragment.....	90
Fig. 31.	MALDI MS of CNBr digest of BPTA cross-linked hemoglobin	94

LIST OF SCHEMES

Scheme 1.	Synthesis of 4-benzyloxy- α -cyanocinnamic acid	40
Scheme 2.	Synthesis of 4-phenyl- α -cyanocinnamic acid	46
Scheme 3.	2'-deoxyguanosine fragmentation pathway	52
Scheme 4.	dGC8AAF fragmentation pathway	57
Scheme 5.	DBSF cross-linking reagent and primary reaction product.....	69
Scheme 6.	Strategy	87
Scheme 7.	BPTA reagent and possible product	92

LIST OF ABBREVIATIONS

α 99XLHb	Hb was cross-linked between α_1 99 Lys- α_2 99Lys by DBSF
β 82XLHb	Hb was cross-linked between β_1 82Lys- β_2 82Lys by DBSF
4HCC	4-hydroxy- α -cyanocinnamic acid
BCC	4-benzyloxy- α -cyanocinnamic acid
BPTA	3,3',4,4'-benzophenone tetra (3,5-dibromosalicylate)
CA	Caffeic acid
CNBr	Cyanogen bromide
DBSF	Bis(3,5-dibromosalicyl) fumarate
DHB	2,5-dihydroxybenzoic acid
DMSO	Dimethyl-d ₅ -Sulfoxide
dG	Deoxyguanosine
dGC8AAF	N-(deoxyguanosine-8-yl)-2-acetylaminofluorene
ESI	Electrospray ionization
FA	Ferulic acid

Hb A	Normal major adult human hemoglobin
HPLC	High performance liquid chromatography
IR	Infrared
PCC	4-phenyl-α-cyanocinnamic acid
MALDI	Matrix assisted laser desorption ionization
MS	Mass spectrometry
NMR	Nuclear magnetic resonance
SA	Sinapinic acid
SDS-PAGE	Sodium dodecylsulfate polyacrylamide gel electrophoresis
TFA	Trifluoroacetic acid
TOF	Time-of-flight
UV	Ultraviolet

LIST OF TABLES

Table 1.	Common matrices	10
Table 2.	Matrices evaluation based on dG and dGC8AAF	58
Table 3.	Matrices evaluation based on bovine insulin	61
Table 4.	Hb β chain tryptic digest fragments	75
Table 5.	Hb α chain tryptic digest fragments	76
Table 6.	Hb α chain tryptic digest fragments corresponding mass value	77
Table 7.	Hb β chain tryptic digest fragments corresponding mass value	77
Table 8.	Hemoglobin A CNBr digest fragments corresponding mass value	82

CHAPTER I

INTRODUCTION

Molecular weight determination is one of the most fundamental measurements necessary for elucidation of the structure of biomolecules. Among the techniques, mass spectrometry has long been one of the best techniques for directly obtaining this information from very small quantities of material. Traditional mass spectrometry is carried out either with electron impact ionization, in which molecules are ionized with an energetic beam (70 eV) of electrons or with chemical ionization, in which volatilized molecules are ionized by reaction with ionic reagent gases. Both techniques required vaporization of neutral moieties followed by ionization. The vaporization process limits the application of mass spectrometry to analyses of small organic compounds. The main difficulties of classical mass spectrometry, if applied to large polar, nonvolatile, and thermal liable substances, have been sample volatilization and sample ionization. During the past decades, tremendous effort has been expended on applying mass spectrometry to very large molecule measurements

for biological and medical application. Several other volatilization and ionization techniques have been successful to varying degrees for molecular weight analysis of larger (up to m/z 5000-10,000 Da) molecules, such as fast atom bombardment (FAB) (Barber et al., 1981), secondary ion mass spectrometry (SIMS) (Mchugh, 1975), field desorption (FD) (Becky, 1977), and plasma desorption (PD) (Macfarlane and Torgerson, 1976). Until the mid 1980s, it was believed that biomolecules larger than 10 kDa could not be ionized or volatilized to enable analysis by mass spectrometry. The breakthrough came with the introduction of electrospray ionization (ESI) (Meng *et al.*, 1988) and matrix-assisted laser desorption ionization (MALDI) (Karas and Hillenkamp, 1988; Tanaka, et al., 1988). These new mass spectrometric methods have enabled molecular weight analyses of biomolecules up to m/z 500,000 (Ehring et al., 1992)

For example, in ESI, highly charged droplets are dispersed from a capillary in a strong electric field at atmospheric pressure. Droplet size is reduced by heat and stream of dry N_2 gas. Ions are expelled by coulombic explosion from the droplets during the evaporation process are then drawn toward an inlet that admits them into the vacuum region of the spectrometer (Fig. 1). Large proteins and oligonucleotides produce multiply-charged ions, brought about by multiple photon transfer events.

An ESI mass spectrum of a sample is characterized by a series of peaks corresponding to ions carrying different charges (and thus exhibiting different mass-to-charge values). The resulting mass spectra must be deconvoluted to determine the molecular weights of the compounds analyzed.

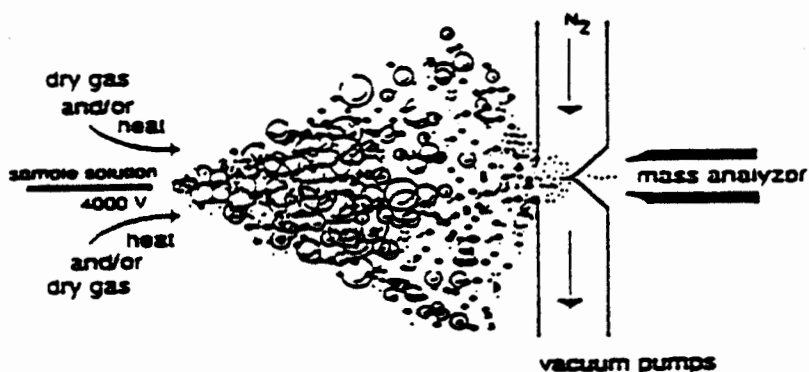


Fig. 1 Electro spray mass spectrometry source (Siuzdak, 1994)

The addition of ESI sources to quadrupole mass spectrometers has extended the accessible mass range up to about 100 kDa (Meng et al., 1988). Electro spray mass spectrometry (ESMS) has made its way into the analytical community and has become an established analytical technique in molecular biology and biotechnology. ESI has gained rapid acceptance due to the ease by which it

could be interfaced with liquid separation techniques (Loo et al., 1989; Mann et al., 1992).

The advent of matrix-assisted laser desorption ionization (MALDI) time-of-flight (TOF) mass spectrometry (MS) occurred during the same time as ESI. Here the analyte of interest is dissolved in a solid matrix, most commonly an aromatic carboxylic acid matrix, that absorbs strongly at the wavelength of the laser that irradiates the sample. The matrix promotes analyte desorption and ionization by preferential absorption of the laser energy which allows the analyte to be absorbed as the matrix sublimates, with little or no fragmentation (Fig. 2).

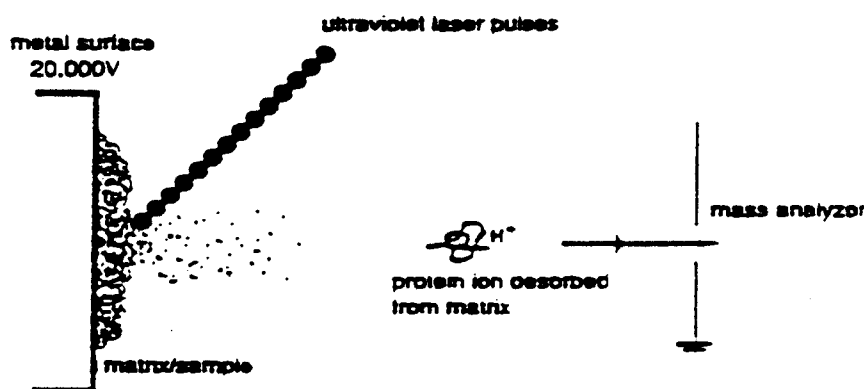


Fig. 2 MALDI mass spectrometry source (Siuzdak, 1994)

MALDI is an ionization technique that is best suited for multichannel mass spectrometers such as time-of-flight (TOF), ion traps, and Fourier transform mass spectrometers (FTMS), because ions are produced in pulses. This technique has extended the accessible mass range up to about 500,000 Da. MALDI is well suited for the analysis of low purity samples (in some instance even natural raw products), could easily perform analysis of complex analyte mixtures. It may be possible to analyze peptides and oligonucleotides directly from blots by MALDI, if the matrix can be incorporated into the sample.

Both ESI and MALDI are so-called soft ionization techniques, which generate protonated molecules of low internal energy generally and thus have little tendency to fragment. Both of these have unique capabilities, as well as some fundamental similarities. In MALDI, ions arise from a solid phase, have low charge states, and can be formed from a sample containing many commonly used biological salts and buffers (Karas et al., 1991; Mock et al., 1992). In contrast, ESI ions are generated from solution, are formed with a range of charge states, and can not be formed efficiently in the presence of even small amounts of extraneous electrolytes (Smith et al., 1991; Kebarle and Tang, 1993). Ions produced by ESI are “colder” than those produced by MALDI and other desorption ionization techniques. Such low internal energy makes these ESI-

generated ions difficult to fragment into product-ion studies. Common feature of these techniques include: generation of unfragmented protonated molecules, the ability to accurately mass analyze biomolecules in the mass range of tens of kilodaltons, detection limits at the low-picomole level. In these respects, the strengths of either the MALDI or the ESI technique complement the weakness of the other.

In this introduction, we will concentrate on MALDI-TOF MS.

1. Development of matrix-assisted laser desorption ionization

Laser ion formation for mass spectrometric analysis dates to the early 1970s (Vastola *et al.*, 1970). Early work combining lasers and mass spectrometry utilized the laser to vaporize neutral species, which were ionized by electron impact (Cotter, 1992). As lasers with short pulse widths and transient digitizers were developed, time-of-flight mass spectrometers could be used to separate the ions ablated during the laser pulse, and in 1975 a laser microprobe mass spectrometer was reported by Hillenkamp (Hillenkamp *et al.*, 1975) for the analysis of biological species. In 1978, Posthumus and coworkers (Posthumus *et al.*, 1978) used a pulsed CO₂ laser and a sector field mass spectrometer to analyze organic compounds. Prior to MALDI, the largest biological molecules produced

by direct laser desorption were m/z 1000. Industrial polymers yield ions as large as m/z 10,000 (Cody, et al., 1990).

In 1988, a major breakthrough enabling the mass analysis of much larger species came about. Independently of each other, the groups of Tanaka (Tanaka *et al.*, 1988) and Hillenkamp (Karas and Hillenkamp, 1988) published mass spectra of monomeric or multimeric organic ions with masses above 100,000. The name matrix-assisted laser desorption ionization mass spectrometry (MALDI-MS), has meanwhile come into use for the method. The Japanese group used metallic nanoparticles suspended in glycerol as a matrix and N_2 laser emitting at 337 nm, whereas the German group used nicotinic acid as a matrix and Nd:YAG laser emitting at 266 nm. Since then, mass spectrometry has been employed effectively in the molecular weight and structural determination of macromolecules. The MALDI technique extended the accessible mass range up to about 500,000 Da at fmol. The mass accuracy at m/z 20,000 is 0.1%.

2. The matrix

The success of MALDI for the sensitive detection of an analyte depends on the nature of the matrix. Since MALDI was first discovered, several different compounds have been employed successfully as matrix. The matrix is a key part

of this mass spectral method. The function of the matrix is generally thought to be three fold (Bahr, et. al. 1994):

- (1) Absorption of energy from the laser light which results in the ejection of both matrix and analyte molecules into the gas phase.
- (2) Isolation of the analyte molecules from each other. Because the analyte molecules are incorporated in a large excess of matrix molecules, strong intermolecular forces are thereby reduced (matrix isolation).
- (3) Ionization of the analyte molecules

The basic rationale to employ matrices for laser desorption ionization was to enable desorption of analytes not resonant with the wavelength of the laser (Karas and Hillenkamp, 1988). In addition, an appropriate matrix candidate should also be fairly water soluble, and not reactive with the analyte. Most useful matrices are found mainly by trial and error because the mechanism of MALDI is still not fully understood. However, some empirical criteria for matrix selection have been suggested (Juhasz, et. al. 1993).

A good matrix substance should at least have the following :

- (1) A reasonable high molar extinction coefficient at the laser wavelength used.

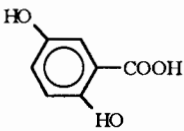
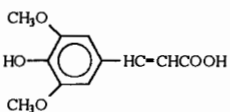
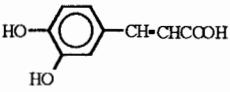
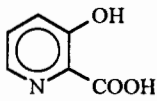
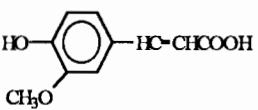
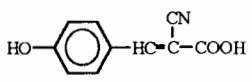
- (2) Miscibility with the analyte in the solid phase and solubility in the same solvents required for dissolution of the analyte.
- (3) Good vacuum stability (low vapor pressure).
- (4) Proper chemical composition that promotes ionization (matrix functional groups that can donate protons to the analyte).
- (5) Nonreactivity with the analyte.
- (6) Other physical properties such as a low heat of sublimation and a capacity to crystallize readily.

A whose host of compounds have been tested as matrix, chosen mainly according to above criteria. Many them were found to work, but only a few became really useful in practice. A list of some common matrices for nitrogen laser is given in the Table 1.

3. Instrumentation

MALDI is a pulsed ionization techniques that is capable of producing ions of high mass and therefore is normally coupled with a time-of-flight (TOF) mass analyzer, although several applications have been performed on FT-ICR (Buchanan and Hettich,1993 and Castoro *et al.*, 1993) or on magnetic sector analyzers (Hill *et al.*, 1991 and Annan *et al.*, 1992); recently using a quadrupole ion trap mass spectrometer have been reported (Jonscher et al., 1993; Lee and Lubman, 1995; Doroshenko and Cotter, 1996).

Table 1.
Common Matrices

Matrix	Structure	References
2,5-Dihydroxy benzoic acid (DHB)		Strupat et al., 1992)
Sinapinic acid (SA)		Beavis and Chait, 1989
3-Hydroxy picolinic acid		Wu et al. 1993
Caffeic acid (CA)		Beavis and Chait, 1989
Ferulic acid (FA)		Beavis and Chait, 1989
4-hydroxy- α -cyanocinnamic acid (4HCC)		Beavis and Chait, 1992

Time-of-flight (TOF) mass analyzer

In TOF analyzers, ions are formed by a pulsed ionization process (pulsed laser radiation for MALDI) in a short source region containing an electric field, the mass-to-charge ratio of an ion is determined by measuring its flight time. After acceleration of the ions in the source to normally the same kinetic energy, they pass a field-free drift tube with a velocity proportional to $(m_i/z_i)^{-1/2}$. Because velocity and mass inversely proportional, ions are separated during their flight. Thus, low mass ions have a shorter flight time than that of heavier ions. The clock (i.e. the oscilloscope) used to measure the TOF of the MALDI ions is triggered by the laser pulse. Typical flight times are a few microseconds (deoxyguanosine) to 100 microseconds (bovine serum albumin). Acceleration voltages are typically 4-30kV and flight path lengths range from 0.5-3m.

All the ions that are formed from a single laser pulse and that are accelerated by the electric field give rise to a transient TOF signal from the detector at the end of the flight tube. Ion detectors as used in other mass spectrometers are either secondary electron multipliers (SEM) or microchannel plates (MCP). Single-shot spectra are usually summed to achieve better signal-to-noise before being transferred to the data system. Time-to-mass conversion is

achieved by incorporating the TOF of ions of known mass (from internal or external standards) into a calibration algorithm from which mass values can be computed for unknown ions with experimentally determined flight times.

There are actually two types of TOF configurations in use for MALDI, linear mode and reflectron mode. Linear instruments represent sort of an archetype which work well for all kinds of parent ions but at moderate mass resolution ($m/\delta m$ no more than 500 normally) (Fig. 3). The more complex reflectron instruments offer a much better mass resolution ($m/\delta m$ more than 2000 for small ions), however, for large molecules, MALDI desorbed ions with poor resolution may observed due to metastable fragmentation. The reflectron mode re-focuses ions according to their energy (Fig. 4).

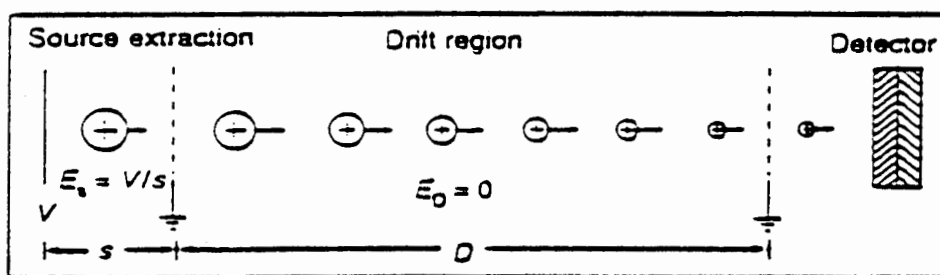


Fig. 3 Diagram of linear mode time-of-flight analyzer (Cotter, 1992)

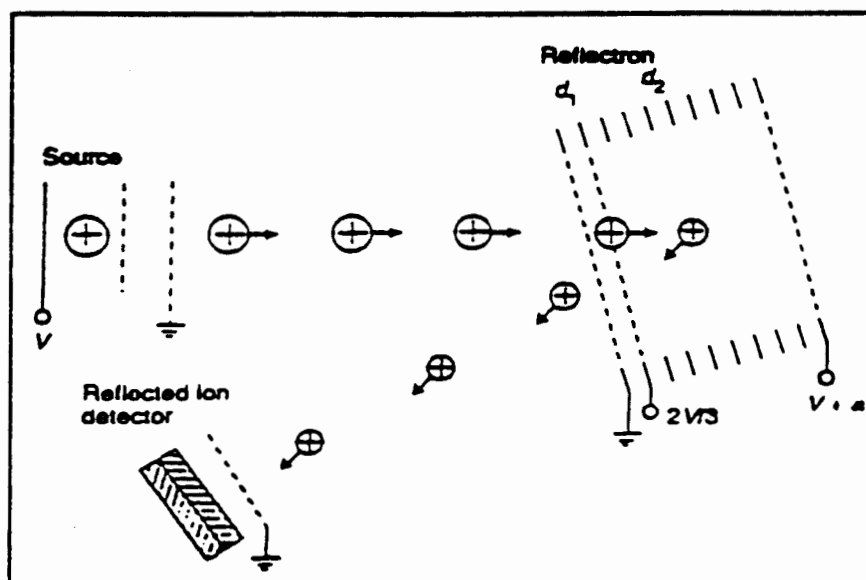


Fig. 4 Diagram of reflectron mode time-of-flight analyzer (Cotter, 1992)

The advantage of MALDI-TOF is that the up mass limit of a TOF analyzer is virtually unlimited, permitting direct determination of very large biomolecules. However, sensitivity decreases with $m^{1/2}$ due to the nature of the detector. Additional virtues of the time-of-flight instrument are high ion transmission, simplicity and low cost. In spite of poor resolving power, MALDI-

TOF can still possibly determine the mass with an accuracy up to $\pm 0.01\%$ (more typically $\pm 0.1\%$) for proteins with molecular mass between 1 to 40 kDa.

4. Applications: Protein Analysis

Identification of protein on the basis of accurate molecular weight determination and peptide mapping is a crucial step in many areas of protein research. The well-established and widely used protein technique such as gel electrophoresis has poor mass accuracy, typically in the range of 5~10% (Hames and Rickwood, 1990). The accuracy of matrix-assisted laser desorption ionization mass spectrometry is much better as described above ($\pm 0.1\%$). The short analysis time, tolerance of impurities, ease of operation, and the price of instrument is changing the way proteins are characterized.

A. Molecular weight determination of proteins

A fundamental parameter in the initial characterization of a protein is to determine its molecular weight. In most biochemical laboratories this is approximated by gel electrophoresis. It is not uncommon, however, to discover large discrepancies between a molecular weight determined by gel electrophoresis and the molecular weight calculated from the amino acid

sequence. This inconsistency led to explore an alternative method, MALDI MS to accurately determine protein molecular weight.

Proteins have turned out to be especially amenable to MALDI analysis, particularly with respect to sensitivity and accessible mass range, and several hundred peptides and proteins have been successfully analyzed. Fig. 5 show a typical MALDI spectrum from cytochrome C (MW 12,384) with 4-Hydroxyl- α -cyano-cinnamic acid (4HCC) (MW 189.2) as matrix, which can serve to demonstrate the main feature of MALDI mass spectrum.

In MALDI mass spectra of cytochrome C, the most intense signal generally is the singly charged molecular ion, in this case, $(M+H)^+ = 12,385$. Additionally, doubly $(M+2H)^{2+}$ and triply $(M+3H)^{3+}$ charged molecular ions as well as singly and multiply-charged cluster ions in some instances. The low mass range (<500 Da) is dominated by background and matrix-related peaks representing species such as monomeric protonated matrix molecules $(4HCC+H)^+ = 189.2$, dimeric protonated matrix molecules $(2 \times 4HCC_2+H)^+ = 379.4$, a protonated decomposition product (dehydration) of the matrix $(4HCC-H_2O+H)^+ = 172.2$, sodium and potassium ions $(M^+) = 23$ and 39 , respectively, as well as other intermittent products. Fig.6 is a mass spectrum of 4HCC.

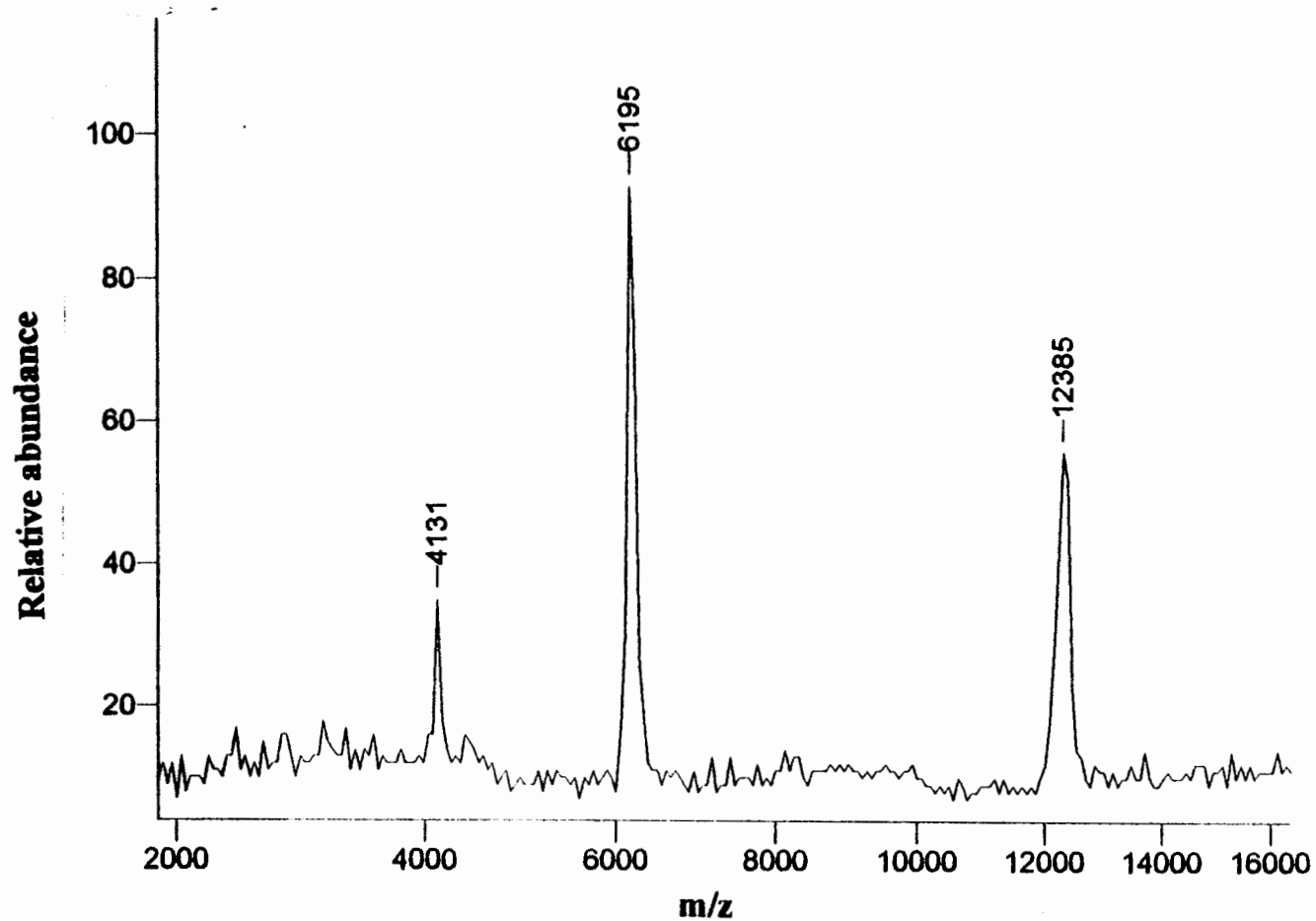


Fig. 5 MALDI MS spectrum of cytochrome C with 4HCC as matrix

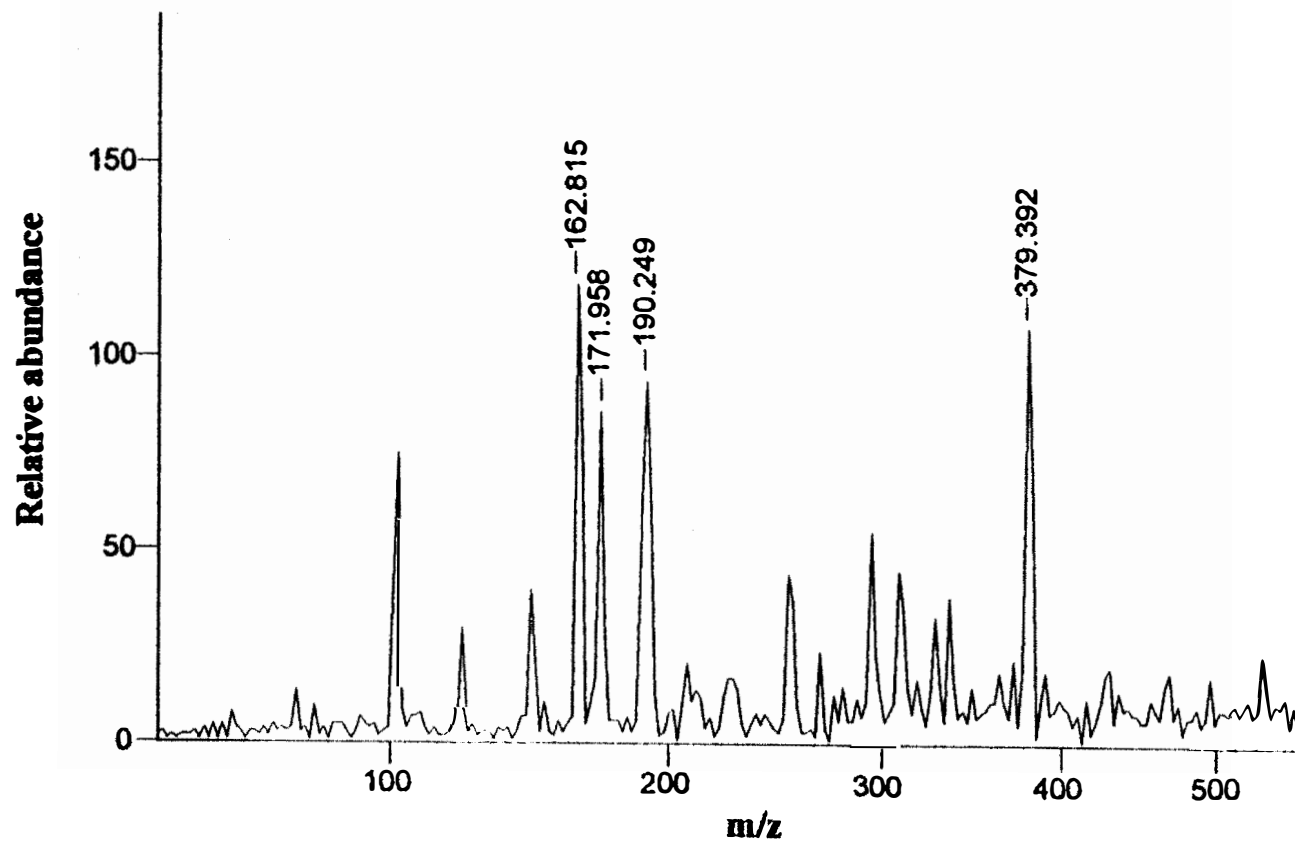


Fig. 6 MALDI MS spectrum of 4-hydroxy- α -cyanocinnamic acid

Proteins undergo protonation (positive ion) or deprotonation (negative ion) are predominant ionization mechanisms. The primary information that can be deduced from these spectra is the molecular masses, which are obtained by taking centroids of the peaks and computing an average value with standard deviation, taking into account the fact that they should all be integer multiples or fractions of each other.

Fragment ions, due to the loss of small neutral molecules such as H_2O , NH_3 or $HCOOH$ from protonated molecular ions, are of low relative abundance. Fragmentation of the amid bonds does not occur during MALDI desorption and ionization.

A mass accuracy of 0.01% for proteins up to 30,000 Da can be obtained (Beavis and Chait, 1989; and 1990). Decrease of mass accuracy in higher mass range is believed to be due to non-resolved adducts between analyte and matrix (Bahr et al., 1994).

B. Structural analysis of proteins

Structural analysis of proteins usually start with the 'identification of a target protein or peptide' in some raw material. Classical methods would require at least some concentration/purification steps before separation (usually

electrophoresis) can give some information on the presence of the compound of interest. Examples are the proteins found in human lipoprotein fraction (Beavis and Chait, 1990), the mapping of saliva enzymes (Nelson and Vestal, 1991), and detection of lactoferrin directly out of a preterm infant urine sample (Hutchens and Yip, 1993).

Traditionally, characterization of proteins is carried out by peptide mapping (Schroeder, 1984) which produced chemical or enzymatic digest followed by separation steps which typically employed reverse phase HPLC with UV detection to identify peptides by their retention time. Mass spectrometry identifies peptide fragments by their molecular weight rather than retention time (Yates et al., 1993; James et al., 1993). In this approach, peptide mass-mapping is performed after cleavage of a protein (of known sequence) at selected sites by specific enzymes or chemical reagents. The calculated peptide masses can be compared to the experimentally observed peptide masses to identify sequence variation or amino acid modification. Again, the ease of operation, the analytic precision, the sensitivity and an only modest degree of selectivity in desorption ionization make MALDI-MS an ideally suited substitute technique for such task. Due to the high tolerance of MALDI for salt and buffer concentration, digest

samples can usually be loaded directly from the reaction vial without purification by chromatography separation (Henzel et al., 1993).

The percentage of fragments observed in a MALDI spectrum depends upon the number of fragments produced in the digest. Therefore, mass mapping more difficult as the molecular weight of the peptide increases. For a protein, in the 10,000 to 15, 000 Da range, MALDI appears to provide quite complete mapping information, usually identifying between 95 to 100% of the fragments (Hancock, 1995). A few investigators have reported on the analysis of tryptic digests of large proteins by MALDI MS i.e. proteins above 25,000 Da. Starting with only 280 fmol of unfractionated material, Billeci and Stults (Billeci and Stults, 1993) measured 24 of 25 expected tryptic fragments of recombinant human growth hormone (rhGH) (MW 22,125), and 45 out of 51 expected glycopeptides from 4.5 pmol digest of recombinant human tissue plasminogen activator (rt-PA) (MW 59,008).

A combination of protein digestion and MALDI-MS peptide mass mapping has been employed successfully in localizing the sites of chemical modification in variety of proteins (Huberty et al., 1993; Robert et al., 1994; Yip and Hutchens, 1992). Since MALDI-MS has 0.1-0.01% accuracy for molecular weight determination, if the target compound is in the mass range below 20 kDa,

the precision and accuracy of molecular mass determination is already good enough to distinguish even small modifications such as phosphorylation (Liao et al., 1994), sulfatation or lipidation (Talbo and Roepstorff, 1993; Spengler et al., 1993). Thus, with target proteins of known structure, MALDI-MS provides for rapid confirmation of structure and information regarding possible modification.

Problem statement

A. Matrices synthesis

We wish to evaluate the utility of two new matrices, 4-benzyloxy- α -cyanocinnamic acid (BCC) and 4-phenyl- α -cyanocinnamic acid (PCC), for the analysis of arylamine-modified nucleotides. This application is suggested by the results of George et al. who demonstrated the utility of these matrices for polycyclic aromatic hydrocarbon (PAH) adducts of nucleic acid at the femtomole level.

The structures of the PAH modified nucleic acids have nonpolar aromatic ring systems on one end and a polar nitrogen heterocycle on the other. Common peptide matrices such as 4-hydroxy- α -cyano-cinnamic acid (4HCC) contain a aromatic ring with polar groups on both ends because peptides possess a number of polar groups. 4-benzyloxy- α -cyanocinnamic acid and 4-phenyl- α -cyanocinnamic acid are similar in structure to adducts because they have a polar group on one end of the molecule and aromatic rings on the other. Moreover, BCC and PCC have strong UV absorption maximum at 334 and 332 nm respectively, which are close to the wavelength of the commonly used nitrogen laser. It is hoped that these two matrices will lower the limits of detection for

DNA adducts, thus enable us to measure the molecular weight for unknown adducts derived from human sources.

B. Identifying cross-linked hemoglobin sites

Cross-linked hemoglobins have been studied for years as potential blood substitutes (Winslow, 1992). However, hemoglobin, free in solution, will not do as a red cell substitute. The reasons for this are rapid clearance by the kidney after dimerization and high oxygen affinity, which prevents adequate tissue oxygenation. Attempts to modify hemoglobin chemically are aimed to overcoming these problems.

In order to develop more effective hemoglobin-based blood substitutes, we must understand the interrelationship between the structure and the products' function. Chemically modification not only change the structure of biomolecule, but also affect the biofunction. By knowing where the modification take place, we can provide insight information about structure. The methods for cross-linking site assignment were based on X-ray crystallography or molecular modeling study. These methods were tedious, time-consuming or lack accuracy.

Here we wish to do peptide mass mapping by MALDI MS as means of characterizing the products of hemoglobin cross-linking reaction.

CHAPTER II

EXPERIMENTAL SECTION

1. Materials and methods

A. Material used for the synthesis of the matrices as follow:

4-hydroxy- α -cyanocinnamic acid and benzyl bromide (Sigma), dimethyl- d_5 -Sulfoxide (DMSO), potassium bromide, ammonium acetate, methanol, benzene, cyanoacetic acid, potassium hydroxide, and 4-biphenylcarboxaldehyde (Aldrich).

B. Materials used for the peptides studies were:

SDS-protein makers, DPCC trypsin, 4-hydroxy- α -cyanocinnamic acid (4HCC), 2,5-dihydroxybenzoic acid (DHB), trifluoroacetic acid (TFA), myoglobin (horse heart), cytochrome C (horse heart), bovine insulin (pancreas), bradykinin, 2'-deoxyguanosine, Bis-Tris purchased from Sigma Chemical Company (St. Louis, MO). Urea, 2-mercaptoethanol, acetonitrile, ammonium citrate, benzoyl chloride, methylene chloride, tetrahydrofuran, formic acid, isopropanol, methanol and ethanol purchased from Aldrich Chemical Company

(Milwaukee, WI). microcon and centricon concentrators from Amicon (Beverly, MA). Hydrochloride acid, methanol, ammonium bicarbonate, acetone, ethyl ether, sodium phosphate dibasic, dialysis tubing, pH standard buffers from Fisher Scientific Company (Fair Lawn, NJ). Phastgel Homogenous 7.5, Phast gel sample applicator 8/1, Phast gel SDS buffer strip, Phast blue R from Pharmacia Chemicals.

C. General methods

Melting points were determined on a Mel-Temp melting apparatus and were uncorrected. Thin layer chromatography (TLC) was conducted on E. Merck aluminum-backed, 0.2 mm silica gel TLC plate. Visualization was accomplished with an ultraviolet lamp (model UVGL-25, Upland, CA).

Proton (^1H) NMR spectra were taken at 300 MHz using a Varian VXR 300 NMR instrument. The chemical shift of the ^1H NMR spectra were referenced to Dimethyl- d_6 -sulfoxide (DMSO) ($\delta = 4.59$). Infrared Spectroscopy data were obtained on a Genesis Series FTIR (ATi instrument North American) in potassium bromide pellets. Ultraviolet spectrum were obtained on a Hewlett-Packard Model 4852A diode-assay spectrophotometer.

High Performance Liquid Chromatography were conducted on a Beckman 421A system with two 110B Solvent Delivery Module pumps, 163 Variable

wavelength detector and 427 Integrator. Centrifugation was carried out on a Sorvall RC5B refrigerated centrifuge using a SS-34 rotor.

2. Synthesis of Matrices

A. 4-benzyloxy- α -cyanocinnamic acid (BCC)

The method for BCC synthesis were adopted from Williamson reaction (Child et al, 1977). Methanol (15 ml) and KOH (0.8 g, 14 mmol) were combined in a round bottom flask and heated until all the KOH dissolved. Then, 4-hydroxy- α -cyanocinnamic acid (0.9 g, 5 mmol) was added to the solution and refluxed. When solution began to boil, benzyl bromide (1.21 g, 7 mmol) was added and the reflux continued for 2 hours. When the reflux was complete, 5 ml of water was added slowly being sure the reaction mixture was still hot. We continued to heat the mixture until the light yellow precipitate dissolved and the solution turned yellow. Then, the reaction was cooled to crystallize the BCC (pale-yellow) from solution. The crystals were collected by vacuum filtration and were washed by cold water. Yield, 33%. Melting Point: 192-196⁰C.

B. 4-phenyl- α -cyanocinnamic acid (PCC)

The method for synthesis of PCC is adopted from Knoevenagel condensation (Astle et al, 1955). 4-biphenylcarboxaldehyde (1.04 g, 5.8 mmol),

cynoacetic acid (0.5 g, 5.8 mmol) and ammonium acetate (0.024 g, 0.3 mmol) were dissolved in 10 ml of benzene, The resulting solution was yellow. The solution was refluxed for eight hours. Then the solution was stirred overnight at room temperature. A green-yellow precipitate was formed and collected by suction filtration. Yield: 52%, Melting point: 241-243⁰C.

3. Preparation for identifying cross-linked hemoglobin sites

A. Preparing the globin chains

All the hemoglobin A and cross-linked hemoglobin solution were from Dr. K. W. Olsen in the chemistry department at Loyola University Chicago and used without further purification. The method we used to prepare globin chains was adopted from the method of Ascoli (Ascoli et al., 1981).

A 5 ml of hemoglobin solution, cooled to 4⁰C, was added dropwise and into 200 ml of acetone (-20⁰C, kept on dry ice) containing 2% concentrated HCl while stirring. After adding the hemoglobin, the acid-acetone solution turned brown, and the globin chains formed a white precipitate. The suspension was centrifuged at 3000 g (-12⁰C) for 10 minutes. The precipitates were collected by suction filtration. The precipitates were washed twice with cold acetone (-20⁰C) in order to remove the residual acid. Then the precipitate was washed by ether and allowed to dry under ambient conditions.

B. Globin chain separation

The globin chain separation were conducted on high performance liquid chromatography (HPLC) by using a Vydac C₄ analytical column (250×4.6 mm). Purified hemoglobin and cross-linked hemoglobin were directly injected to the HPLC. The buffer A was 20% acetonitrile, 80% water in 0.1% trifluoroacetic acid (TFA), buffer B was 60% acetonitrile, 40% water in 0.1% TFA. The gradient was as follow: buffer B from 50 to 62.5% over 60 minute period, 62.5 to 86% over 20 minute period, then back to 50% over 10 minute period.

C. Conversion of myoglobin to apomyoglobin

Removal of the heme was accomplished in a manner similar to the removal of the heme from hemoglobin with minor modification. Dry myoglobin was dissolved in a minimum volume of distilled deionized water. The apomyoglobin was precipitated by dropwise addition of the myoglobin solution to a 100-fold excess volume of ice-cold, rapidly-stirring acetone in 0.3% HCl. The apomyoglobin was allowed to settle on ice for 15 minutes and pelleted with a centrifuge (3000 g). The supernatant was removed and the pellet was washed once with ice-cold acetone in 0.3% HCl, the residual acetone was blown off

under a stream of helium. The apomyoglobin was dissolved in 1:1 acetonitrile + water and dried thoroughly in a speed vac.

D. Sodium Dodecylsulfate Polyacrylamide Electrophoresis (SDS-PAGE)

The SDS-PAGE gel electrophoresis was carried out on a Pharmacia PHAST gel apparatus. 12.5% of homogeneous gel (12.5% T, 2% C) and buffer strips (Pharmacia Co.) were used. The samples were denatured for 5 minutes at 100°C in 10 µl of a solution made of 0.25M Tris, pH=6.8, 4% of SDS, 20% of glycerol, 10% of β-mercaptoethanol and 0.05% of bromophenol blue as the marker dye. One set of molecular weight standard marker was used. The protein molecular weight standard markers were bovine albumin (66,000 daltons), egg albumin (45,000 daltons), glyceraldehyde-3-phosphate dehydrogenase (29,000 daltons), carbonic anhydrase (24,000 daltons), trypsin inhibitor (20,100 daltons) and α-lactalbumin (14,200 daltons). The molecular protein standard markers were treated in the same digestion mixture as the samples. Electrophoresis was carried at a constant current of 10mA (250V until the marked dye reached the bottom of the gel). After the electrophoresis, the proteins were fixed and stained by soaking the gel in 0.1% of PhastGel blue R solution in 30% of methanol and 10% of acetic acid in distilled water for 5 minutes. The gel was destained in 30% of methanol and 10% of acetic acid in distilled water for 20 minutes twice.

The molecular weight of the separated α , β -globin chains were estimated from the graph of the log of molecular weight versus relative mobility of the standard markers.

E. Enzymatic digestion

Digestion of bovine insulin

Tryptic digestion of bovine insulin method was from (Vestling, 1991 and Matsudaira, 1993). Trypsin was dissolved in 0.1mM CaCl_2 solution to make 1mg/ml stock solution. Bovine insulin was dissolved in 0.1M NH_4HCO_3 , 0.1mM CaCl_2 buffer to make 1mg/ml solution. 20ml of trypsin solution(1g/ml) were added to 1ml of bovine insulin solution, vortex for a few minutes, incubated in 37°C for 2 hours, then boiled sample for 2 minutes and keep in freezer for MS analysis.

Tryptic digestion of apomyoglobin

The apomyoglobin was dissolved at concentration approximately 0.5 nmol/ μl in 2M of urea, 0.1M of Tris-HCl (pH=8.3), and digested with 2% by weight of trypsin for 3 hours at 37°C .

Digestion of hemoglobin

Digest of Hb with trypsin were adopted from Kluger et al (1992). Heme-removed hemoglobin and myoglobin were dissolved in 8M urea and keep at room temperature for 2-4 hours to increase susceptibility to digestion. The solution was diluted to 2M urea with 80mM ammonium bicarbonate buffer, pH was 8.5. Trypsin was dissolved in 80mM ammonium bicarbonate to make 1mg/ml stock solution and 5% of total protein weight's trypsin were added to globin chains solution. The globin chains digested for 24 hours at room temperature. The tryptic peptides were then boiled for 2 minutes, keep in freezer and ready for MS analysis.

CNBr digestion of hemoglobin or cross-linked hemoglobin was performed by Dr. Kondubhotla.

F. Centricon (or micron) isolation

After enzymatic digestion, 300 μ l samples were placed in microcons and then centrifugeed in a savant speed vac for overnight. The membranes were washed with 0.1% TFA water solution several times.

For CNBr digestion of cross-linked hemoglobin, we used centricon to isolate the fragment we were interested. One to 3 ml of digested cross-linked

hemoglobin solution was placed in a centricon, centrifuge at 3000g for 30 minutes, and washed with 2M urea a few times.

G. Peptide Mapping by High Performance Liquid Chromatography (HPLC)

Tryptic peptides were mapped by HPLC on a Vydac C₁₈ column / at a flow rate at 1ml/min. For bovine insulin, we used gradient from 10% to 50% acetonitrile in 0.1% trifluoroacetic acid (TFA) over 20-min period. In this system there complete separation of the tryptic peptides. For myoglobin, the gradients used were from 0 to 10% over 10-min period and then 10-50% acetonitrile with 0.1% TFA over 20-min period. The Buffer A for these two systems were 0.1% TFA in water. For hemoglobin, we used gradient from 0 to 15% B over 10 minutes, 15-50% over 60 minutes, and then 55-100% over 10 minute. (A = 0.1% TFA, B = 80% acetonitrile, 0.1% TFA).

Collected effluents were evaporated to dryness by speed vac, then matrix solution was added directly to dried sample vial, and the sample was subject to MS analysis.

4. MALDI-TOF MS

A. Instrument set up

The MALDI-TOF Mass spectrometer constructed at Loyola University Chicago was a modified Wiley-McLaren design (Model D850, manufactured by R. M. Jordan Co., Grass Valley, CA) and may be operated either in the linear or reflectron mode. A nitrogen laser (VSL 337 ND, Laser Science Inc., Cambridge, MA) is used to induce desorption and ionization. The wavelength of the laser is 337nm and pulse width is 3 nanosecond. Fig. 7 is the diagram of the instrument. The ionization region is housed in a cubic stainless steel vacuum chamber pumped with a turbo pump (turbo-250V, Model 969-9423, Varian, CA), and this pump is also connected to another turbo located at middle of the flight tube. The flight tube is made from stainless steel tube, providing a total flight path of 1 m. The vacuum pressure of the instrument in the flight tube is $10^{-6}\sim 10^{-7}$ torr. The intensity of laser beam was controlled by a variable-beam attenuator (Newport Corp., Fountain Valley, CA) and focused onto the probe tip at a 45° angle to the probe surface with a single focal length quartz lens to a spot size of $150\mu\text{m}$. The product ions were accelerated with potential 20kV and were allowed to drift down a field free region held in a vacuum maintained below 10^{-5} Torr. The acquisition of mass spectrum is initiated by the firing of the laser. A small fraction of the light is reflected off the laser optics as the light pulse enters the mass spectrometer. This reflected light strikes the surface of a photodiode which triggers the digital oscilloscope (Model TDS 520A, Tektronix, Beaverton, OR)

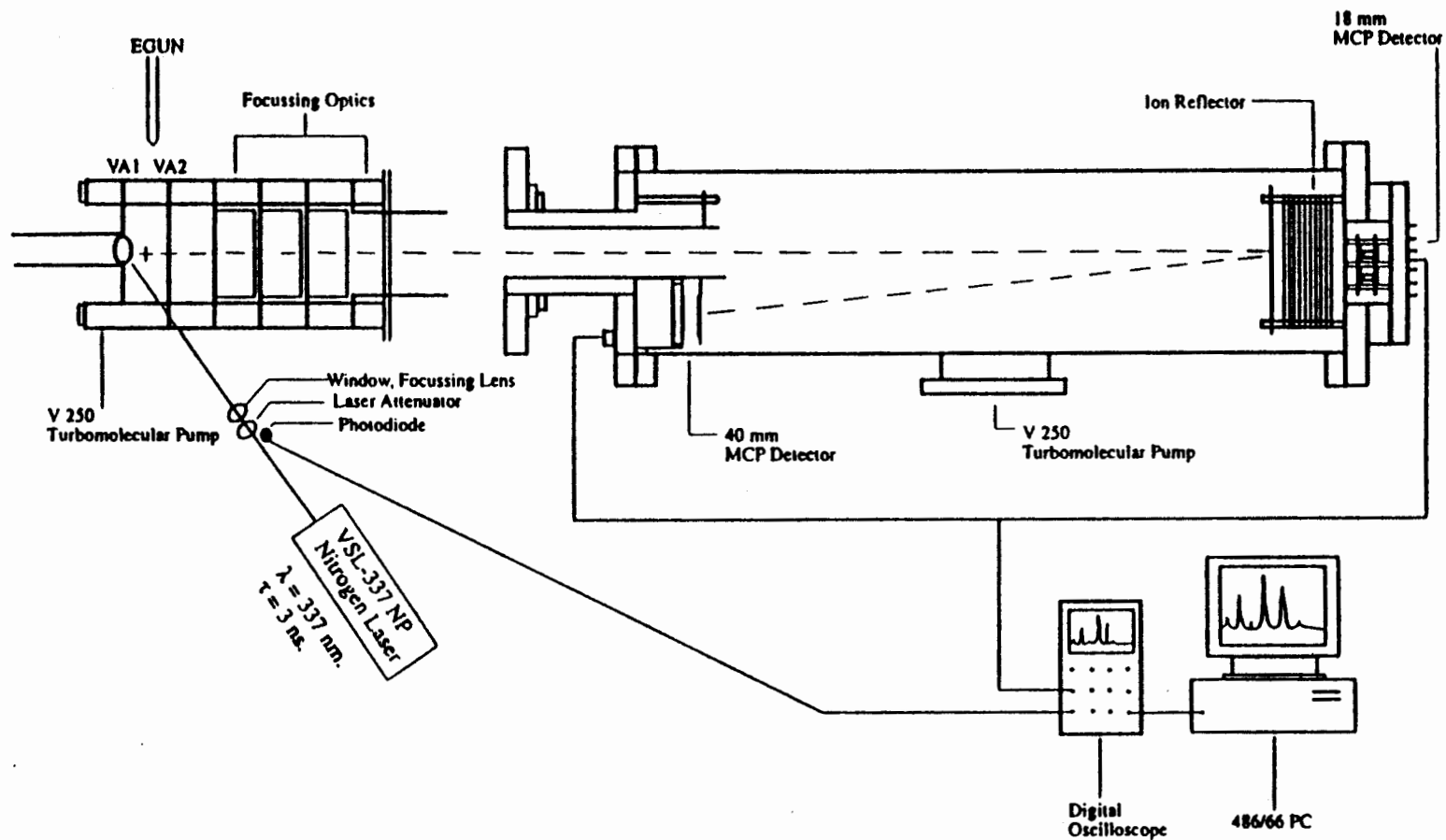


Fig. 7 Scheme of MALDI-TOF instrument used in experiment

to initiate data acquisition. The detector is a 18 mm diameter dual-layer microchannel plate (MCP) detector. Data were recorded using a Tektronix digital oscilloscope and subsequently transferred to an IBM 486 compatible PC for processing. Spectra consisted of a summation of 20 to 30 laser shots. Spectra calibration and peak centroids were carried out on a 486 PC using TOFWARE software.

B. Sample preparations

Peptides used as external standard were prepared by dissolving the peptides in 0.1% TFA/water to make solution concentration of 1mg/ml. Digested samples either used as it was or prepared by centricon separation first. Some commonly used matrix materials, including 2,5-dihydroxybenzoic acid (DHB), caffeic acid (CA), sinapinic acid (SPA), 3-hydroxypicolinic acid (HPA), 4-hydroxy- α -cyanocinnamic acid (4HCC) were obtained from Aldrich Chemical Co., and used without further purification. Near-saturated matrix solutions or 50mM of 4HCC were prepared with 1:2 (v/v) deionized water and acetonitrile with 0.1% trifluoroacetic acid.

Samples were prepared by either premix sample and matrix or sequentially load sample and matrix on probe tip.

For premix sample, mixing a 2 μ l aliquot of sample solution with 20 μ l of matrix solution, vortex a few minutes. A 1 μ l of the mixture was loaded on stainless probe tip and allowed to air dry at room temperature prior to introduce into the mass spectrometer.

Sequentially loading sample and matrix on probe tip were from Vorm et al (1994). Matrix was dissolved in acetone to make a saturated solution. The matrix solution were applied on probe first, air dried, then the sample was put on top of matrix layer.

The nafion film method of Bai et al.(1994) was also used. Nafion is available in liquid form at a concentration of 5% in a mixture of 10% water and lower aliphatic alcohols. Approximately 5 μ l of this solution was applied to the stainless steel probe tip and air dry. Nafion formed a thin layer of film. The sample was directly deposited on the film and then the matrix was sequentially load onto the probe.

External calibration was performed using either mixture of bradykinin (MW 1060.27) and bovine insulin (MW 5733.5), or mixture of cytochrome C (MW 12,384) and myoglobin (MW 16,951).

CHAPTER III

SYNTHESES AND EVALUATIONS OF MATRICES

The search for useful matrix compounds has been an active area of MALDI MS research since the birth of the technique. Several hundred different organic compounds selected based on their UV absorbance (wavelengths at 337 for N₂ laser or 355nm for Nd:YAG laser) have been investigated. However, only a few of these are widely applicable. Most of the useful matrix compounds for peptides reported to date have been highly substituted, aromatic compounds containing carboxylic acid moieties. The requirement for aromaticity stems from the existence in such compounds of an absorption band close to the laser wavelengths commonly used for MALDI analysis. However, the role and /or importance of acidic functional groups during ionization in the MALDI process has not been established. Since the mechanism of MALDI is not fully understood, new matrices are still usually found by trial and error.

The application of the technique to the mass analysis of nucleic acids has not been straightforward. The acidic matrices commonly used for the MALDI analysis of proteins have not been found to be generally applicable to analysis of

oligonucleotides and related compounds. Some empirical criteria for matrix selection have been proposed (Juhasz et al., 1993), however, George and coworkers proposed that the matrix which has similar structure to the particular analyte should give the best results. They reported two new matrices, 4-benzyloxy- α -cyanocinnamic acid (BCC) and 4-phenyl- α -cyanocinnamic acid (PCC) that allowed for the detection of polycyclic aromatic hydrocarbon (PAH) modified nucleic acids (DNA) adducts at low femtomole level. We have test these matrices for the analysis of C8-substituted arylamine adducts of deoxyguanosine.

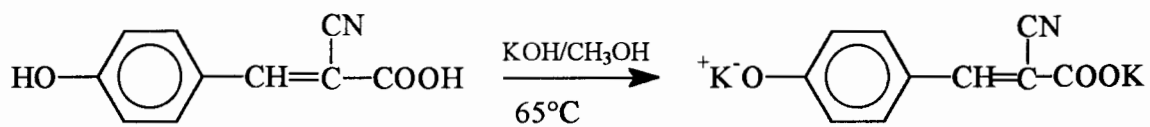
It is hoped that these matrices will enable lower limits of detection for arylamine nucleoside adducts, thus enable the molecular weight measurement of otherwise unknown adducts derived from human sources.

1. Synthesis of matrices

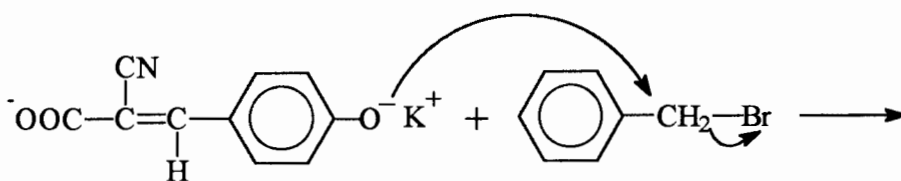
A. 4-Benzyloxy- α -cyanocinnamic acid 3

4-Hydroxy- α -cyanocinnamic acid (4HCC) 1, one of the most commonly used matrix for MALDI, was deprotonated first by using 1M of potassium hydroxide in methanol at 65^oC. Under basic condition, 4-hydroxy- α -cyanocinnamic acid was refluxed with benzyl bromide 2 (refer to Chapter II).

Since acid may break ether $-\text{OCH}_2-$ bond, we did not acidify the product. The reaction gave a moderate yield (33%). The product was recrystallized from acetone. However, prior literature listed 4-benzyloxy- α -cyanocinnamic acid melting point was $204\text{-}205^\circ\text{C}$ (George et al., 1994), we didn't get this melting point even after recrystallization with acetone. Our melting point was $192\text{-}196^\circ\text{C}$. Evidence of 4-benzyloxy- α -cyanocinnamic acid **3** formation is supported by the present of $-\text{CH}_2\text{O}-$ group between two benzene ring in ^1H NMR (at $\delta = 5.26$). The ^1H NMR spectra of 4-benzyloxy- α -cyanocinnamic acid in DMSO is shown in Fig. 8, and chemical shift for H^1 are : $\delta 5.26$ (s, 1H), $\delta 7.27$ (d, 2H), $\delta 7.38\text{-}7.43$ (m, 3H), $\delta 7.50\text{-}7.525$ (d, 2H), $\delta 8.09\text{-}8.12$ (d, 2H), $\delta 8.24$ (s, 1H). The NMR spectrum indicated some impurities in the sample. Also, the UV spectrum Fig. 9 has an absorbance maximum at 334 nm consistent with the literature (George et al. 1994). IR spectra (Fig. 10) showed evidence (1239 cm^{-1} for asymmetric C-O-C stretch) for $-\text{CH}_2\text{O}-$ group linkage. Positive ion MALDI spectra (Fig. 11) did not show abundant $(\text{M}+\text{H})^+$ molecular ion of m/z 280 (calculated $\text{C}_{17}\text{H}_{12}\text{NO}_3$, 278), but showed $(\text{M}+\text{K})^+$ ion of m/z 318 and $(\text{M}+\text{K}-\text{H}_2\text{O})^+$ ion of m/z 301 which indicated synthesis was successful.

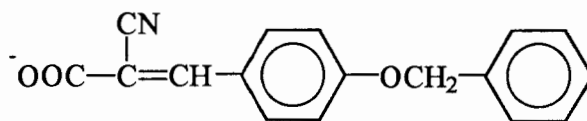
4-hydroxy- α -cyanocinnamic acid

1



benzyl bromide

2

4-benzyloxy- α -cyanocinnamic acid

3

Scheme 1. Synthesis of 4-benzyloxy- α -cyanocinnamic acid 3

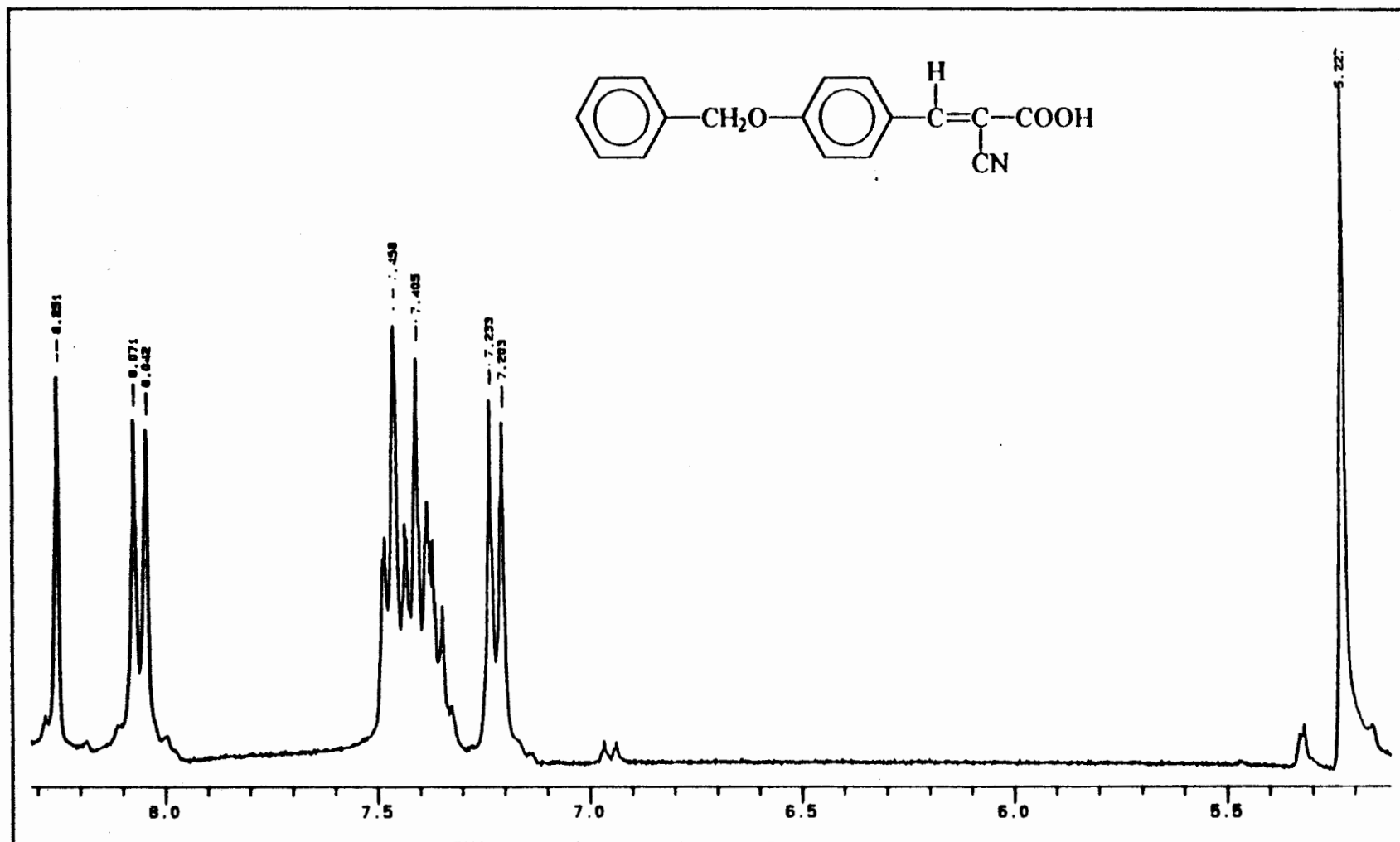


Fig. 8 NMR spectrum of 4-benzyloxy- α -cyanocinnamic acid

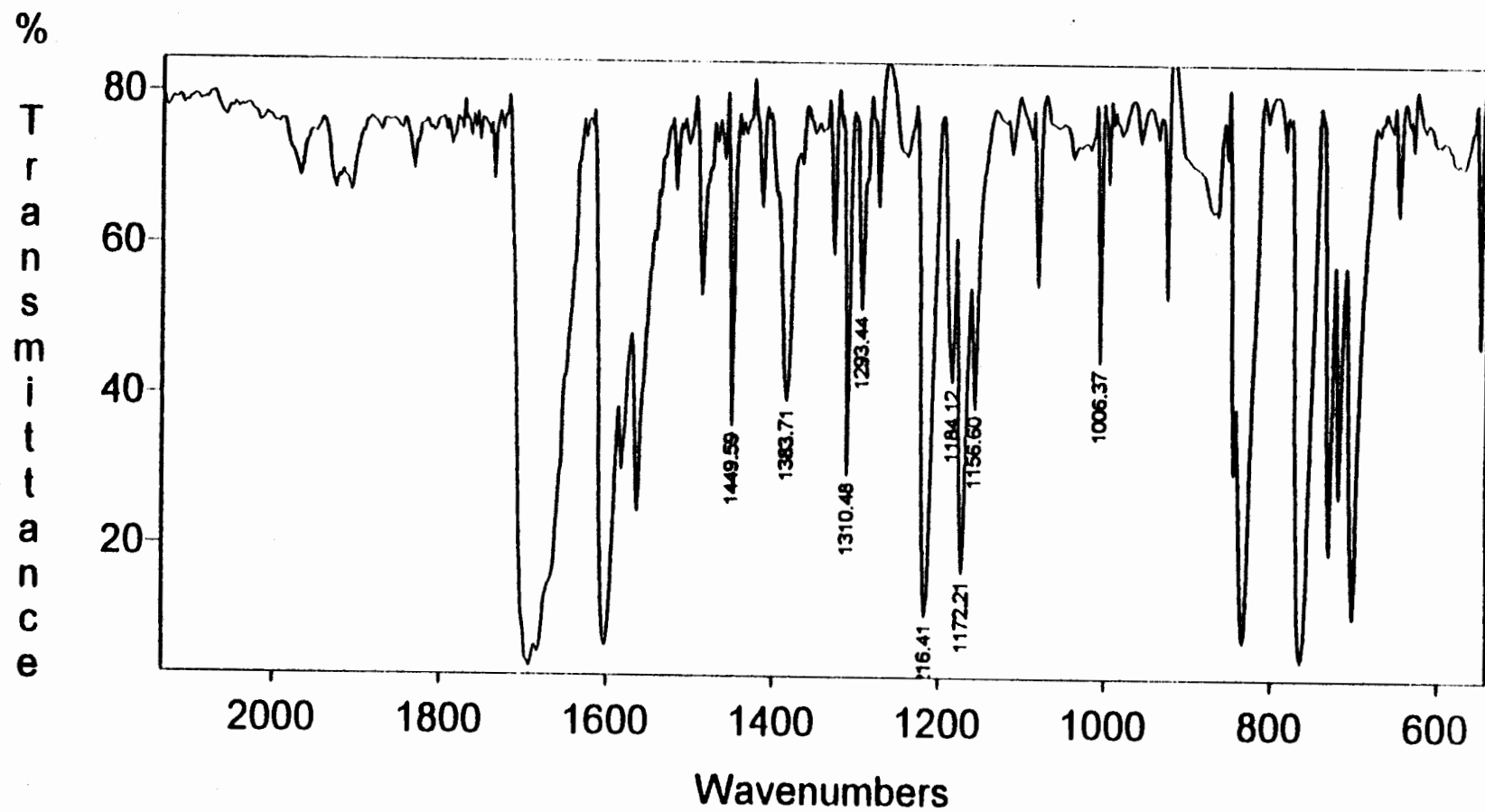


Fig. 9 IR spectrum of 4-benzyloxy- α -cyanocinnamic acid

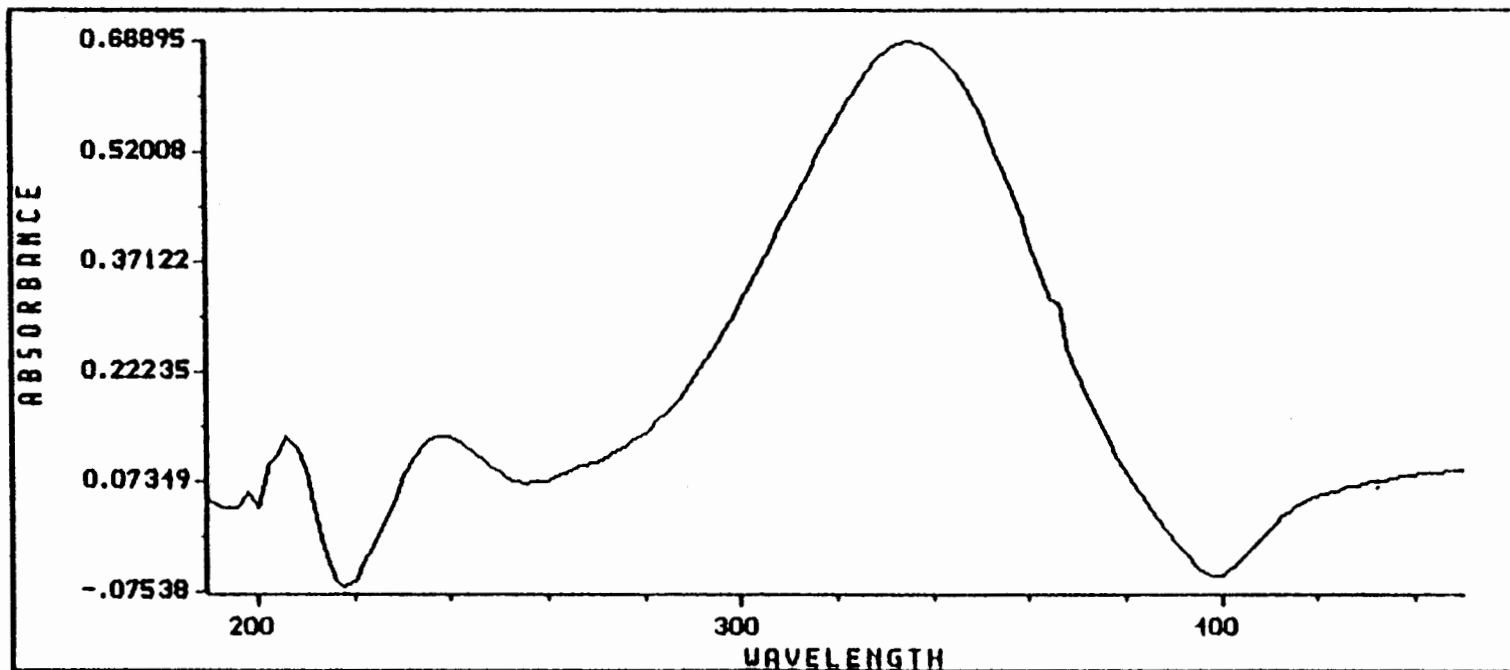


Fig. 10 UV spectrum of 4-benzyloxy- α -cyanocinnamic acid

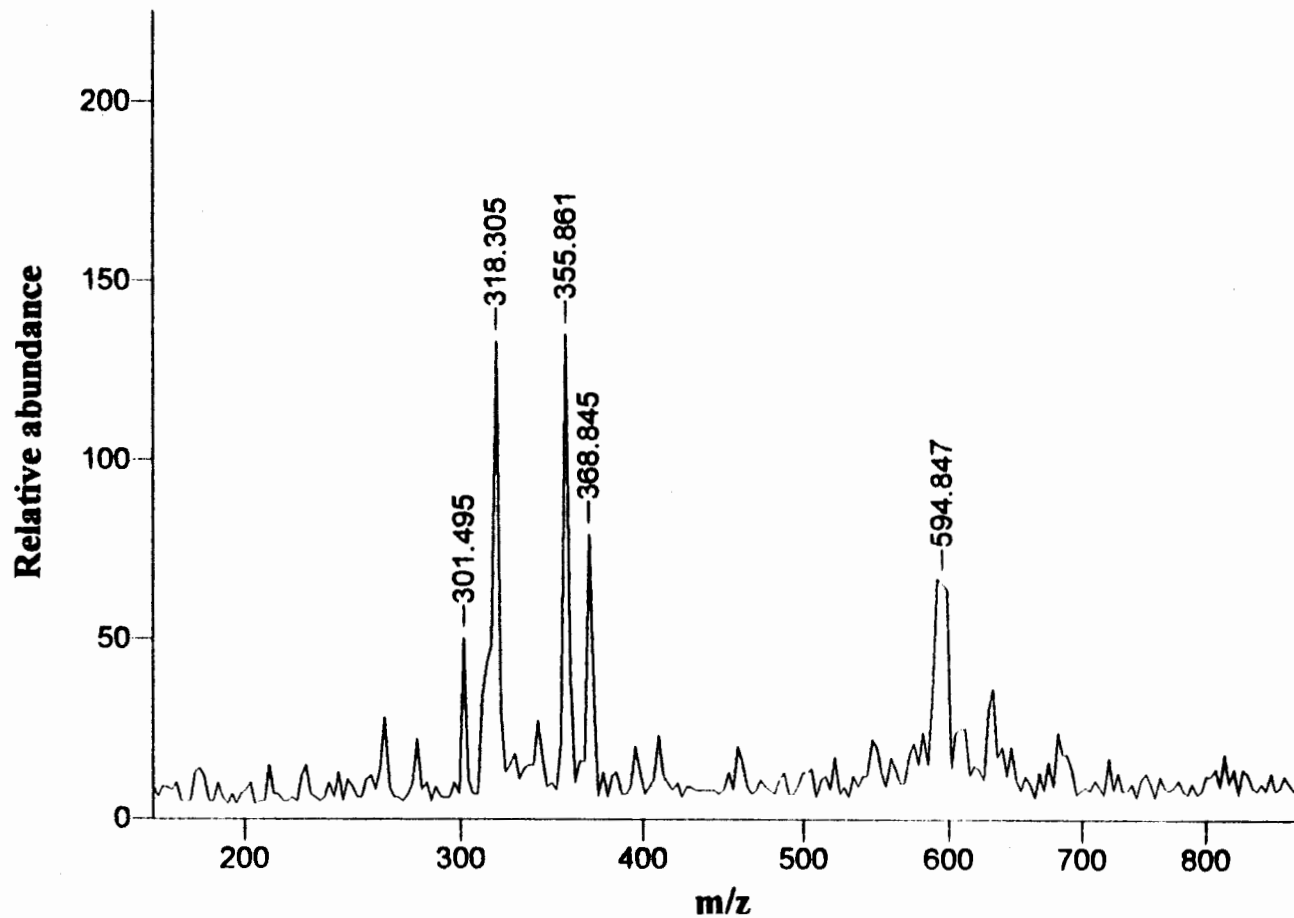
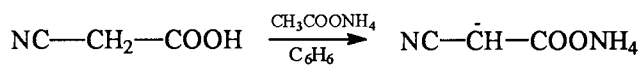


Fig. 11 MALDI MS spectrum of 4-benzyloxy- α -cyanocinnamic acid

B. 4-phenyl- α -cyanocinnamic acid 7

Cyanoacetic acid **6** was deprotonated using ammonium acetate **8** in benzene from room temperature to approximately 78⁰C. Commercially available 4-phenyl- α -cyanocinnamic acid **7** was added to this solution, and brought to reflux (refer to Chapter II).

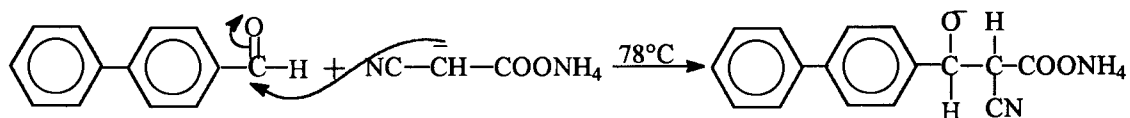
The product was a yellowish green powder after washing with cold water. The yield was 52%. The ¹H NMR spectra showed chemical shift at $\delta = 8.37$ indicated the formation of bond between -C=CH- group and biphenyl group. Fig. 12 showed ¹H NMR spectrum of 4-phenyl- α -cyanocinnamic acid in DMSO, and the chemical shift for H¹ are: δ 7.40-7.55 (m, 3H), δ 7.75-7.80 (D, 2H), δ 7.87-7.95 (d, 2H), δ 8.17-8.22 (d, 2H), δ 8.37 (s, 1H). The chemical shift at $\delta = 2.49$ was solvent DMSO. The melting point (241-243⁰C) was consistent with the literature (George et al., 1994). UV spectra (Fig. 13) supported the formation of 4-phenyl- α -cyanocinnamic acid by showing absorbance maximum at 332 nm. The IR spectra (Fig. 14) of this compound gave a peak around 2200cm⁻¹ confirming the presence of the -CN functional group. Positive MALDI spectra of PCC (Fig. 15) showed abundant (M+H)⁺ ions of m/z 249 (calculated for C₁₆H₁₀NO₂, 248) and (M+H-H₂O)⁺ ion of m/z 232. The ion at m/z 268 was (M+NH₃)⁺.



Cyanoacetic Acid

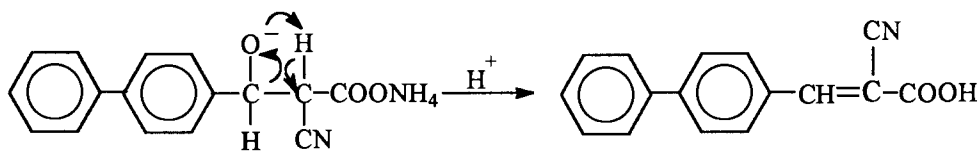
4

5



4-biphenylcarboxaldehyde

6

4-phenyl- α -cyanocinnamic acid

7

Scheme 2. Synthesis of 4-phenyl- α -cyanocinnamic acid

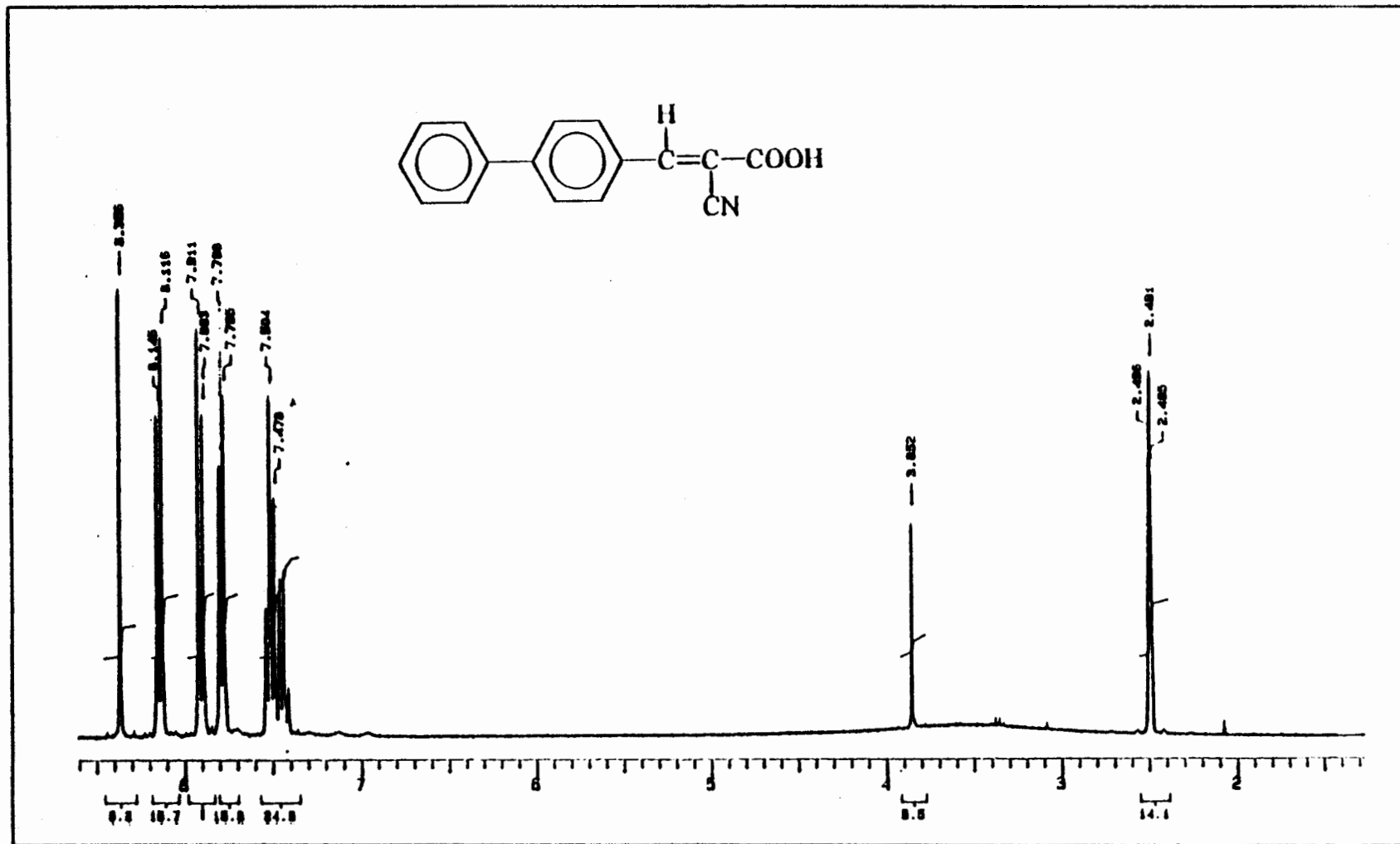


Fig. 12 NMR spectrum of 4-phenyl- α -cyanocinnamic acid

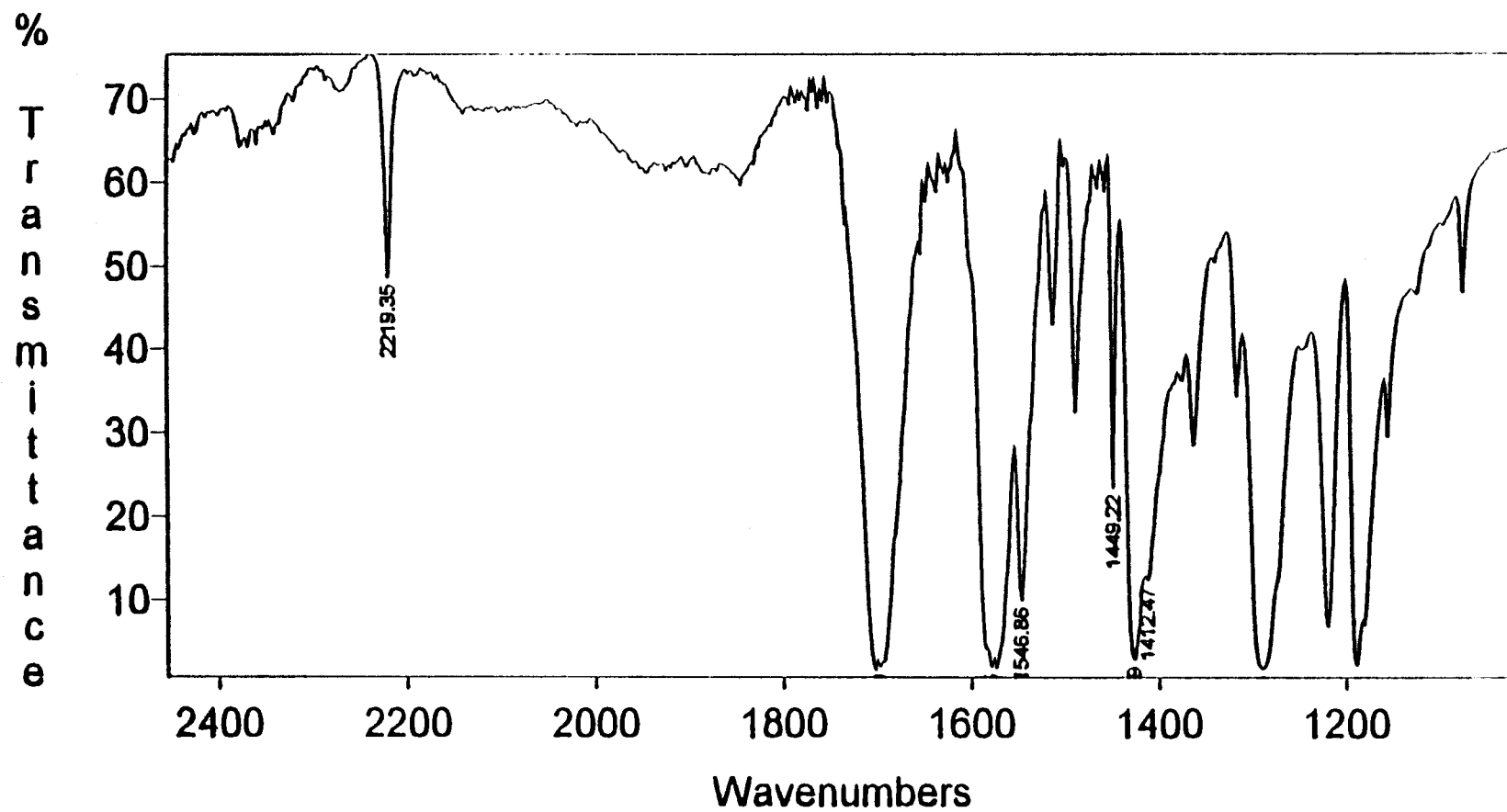


Fig. 13 IR spectrum of 4-phenyl- α -cyanocinnamic acid

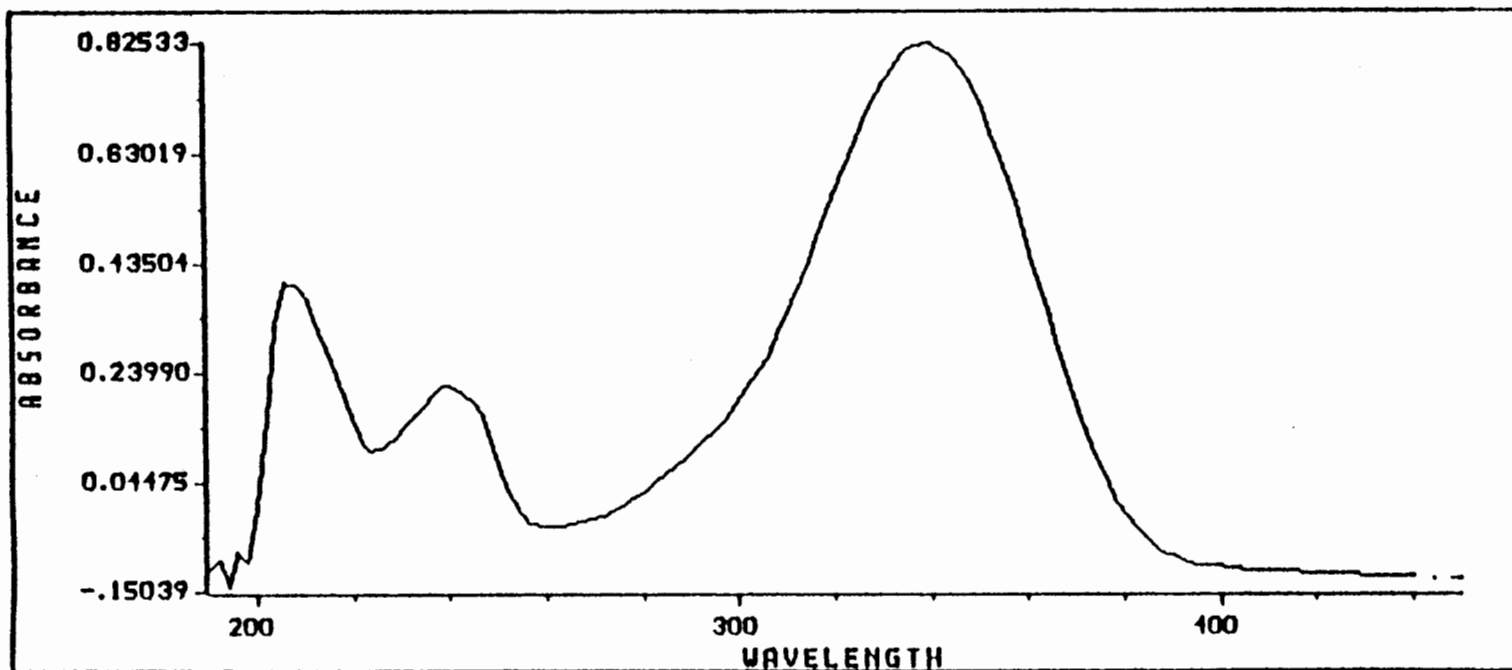


Fig. 14 UV spectrum of 4-phenyl- α -cyanocinnamic acid

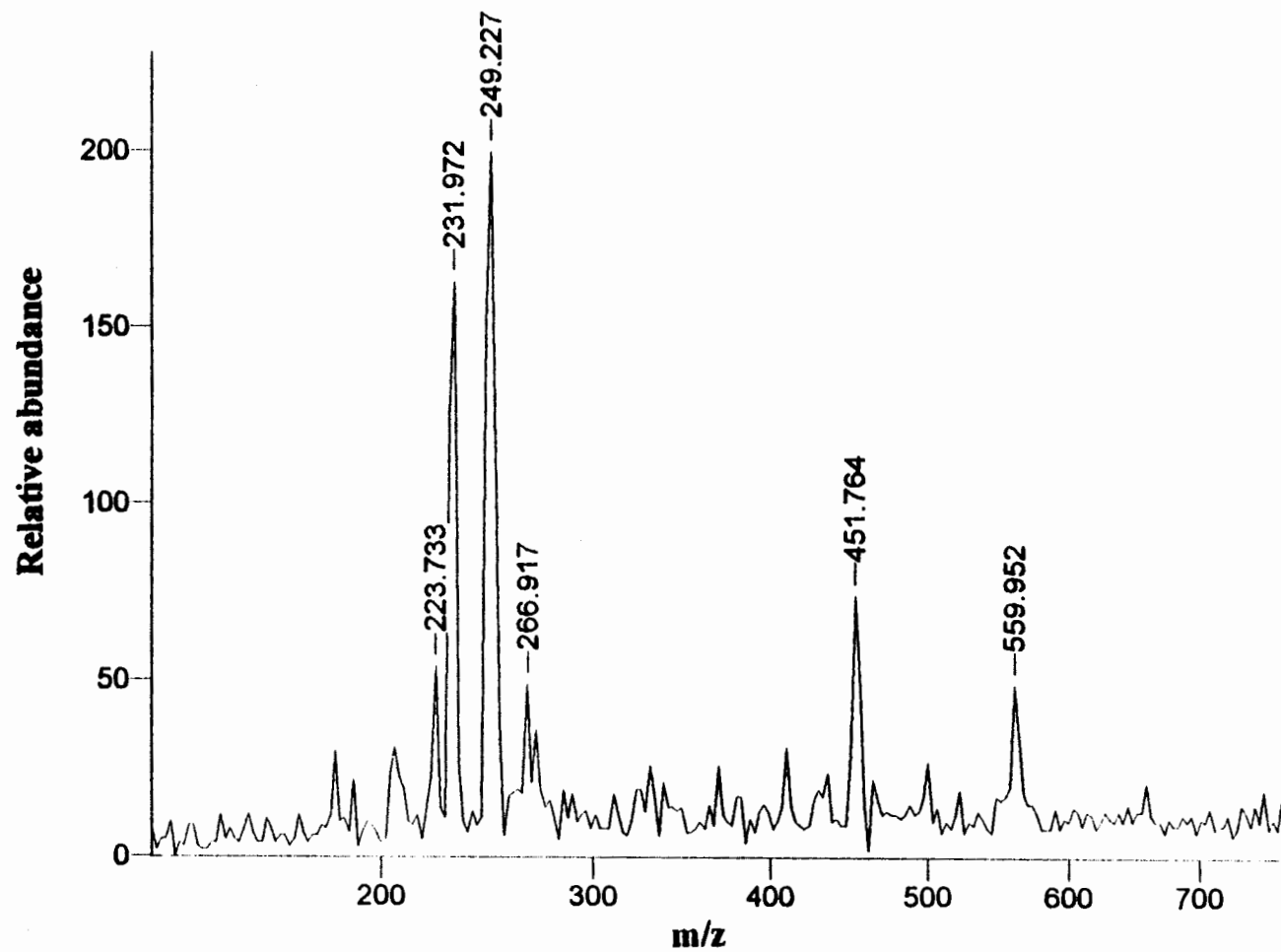


Fig. 15 MALDI MS spectrum of 4-phenyl- α -cyanocinnamic acid

2. Matrix evaluation

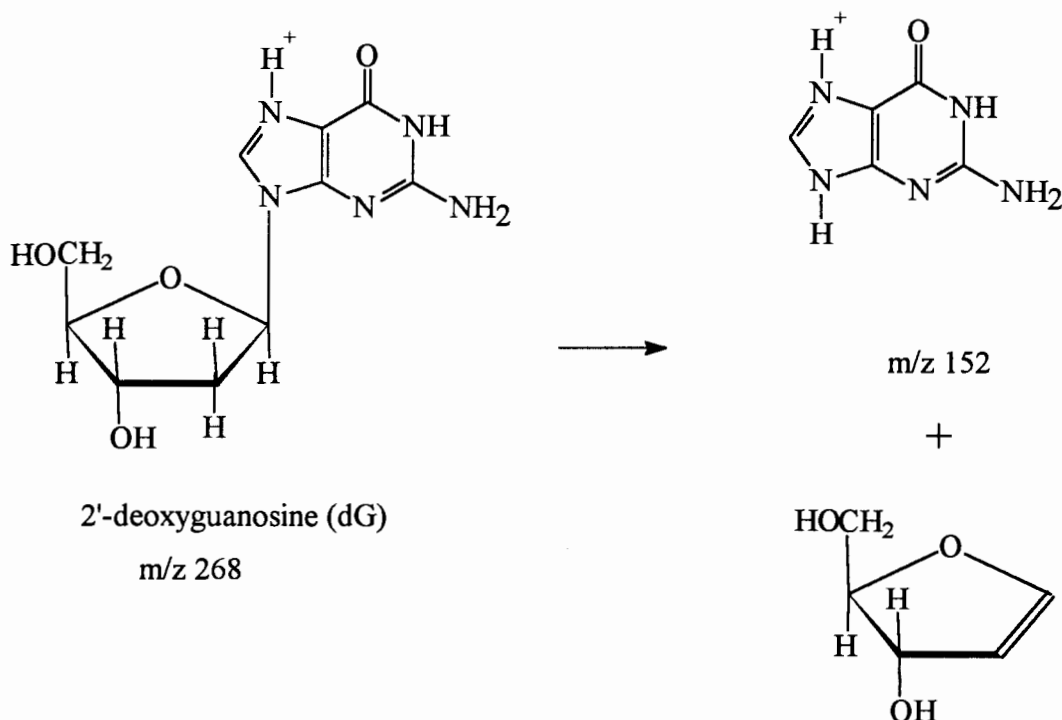
A. Deoxynucleoside Adduct Studies

In order to compare BCC, PCC with other matrix, we examined BCC, PCC and 4HCC resolution and detection limits based on 2'-deoxyguanosine (dG) and N-(deoxyguanosin-8-yl)-2-acetylaminofluorene (dGC8AAF).

It was not possible to use calibration plots to determine the limits of detection because the signals produced by MALDI were highly variable. The lowest amounts of analytes required for reproducible observation of their molecular ion (signal to noise ratio at least 3:1) for there sample loading were taken as detection limits. These limits were established by loading progressively lower and lower amounts of analyte. Matrix blanks were run to identify the matrix peaks that might obscure an analyte peak. We have observed that 2'-deoxyguanosine did yield observable signals from 4-hydroxy- α -cyanocinnamic acid (4HCC), 4-benzyloxy- α -cyanocinnamic acid (BCC), and 4-phenyl- α -cyanocinnamic acid (PCC).

The MALDI-TOF mass spectrum of dG (Fig. 16) obtained by using 35 picomole of the analyte, showed an abundant (M+H)⁺ ion of m/z 268 for 4HCC (A) and BCC (B), but PCC(C) had peak at 268 which interference with the dG peak. Another ion at m/z 152, formed by the loss of deoxyribose, was observed in all spectra. The detection limit for dG was found to be 3.5 pmol based on the

m/z 152 peak (see Table 2) for these matrices. The mass resolution was $m/\Delta m$ at full width of half maximum (FWHM)



Scheme 3 2'-deoxyguanosine fragmentation pathway

The MALDI MS analysis of dGC8AAF adduct spectra (10 pmol) are given in Fig. 17 with 4HCC (A), BCC (B), and PCC (C) as matrix respectively. We did not observe $(M+H)^+$ ion of m/z 489 in any of these matrices. However, an ion at m/z 373 corresponding to loss of the deoxyribose was observed in

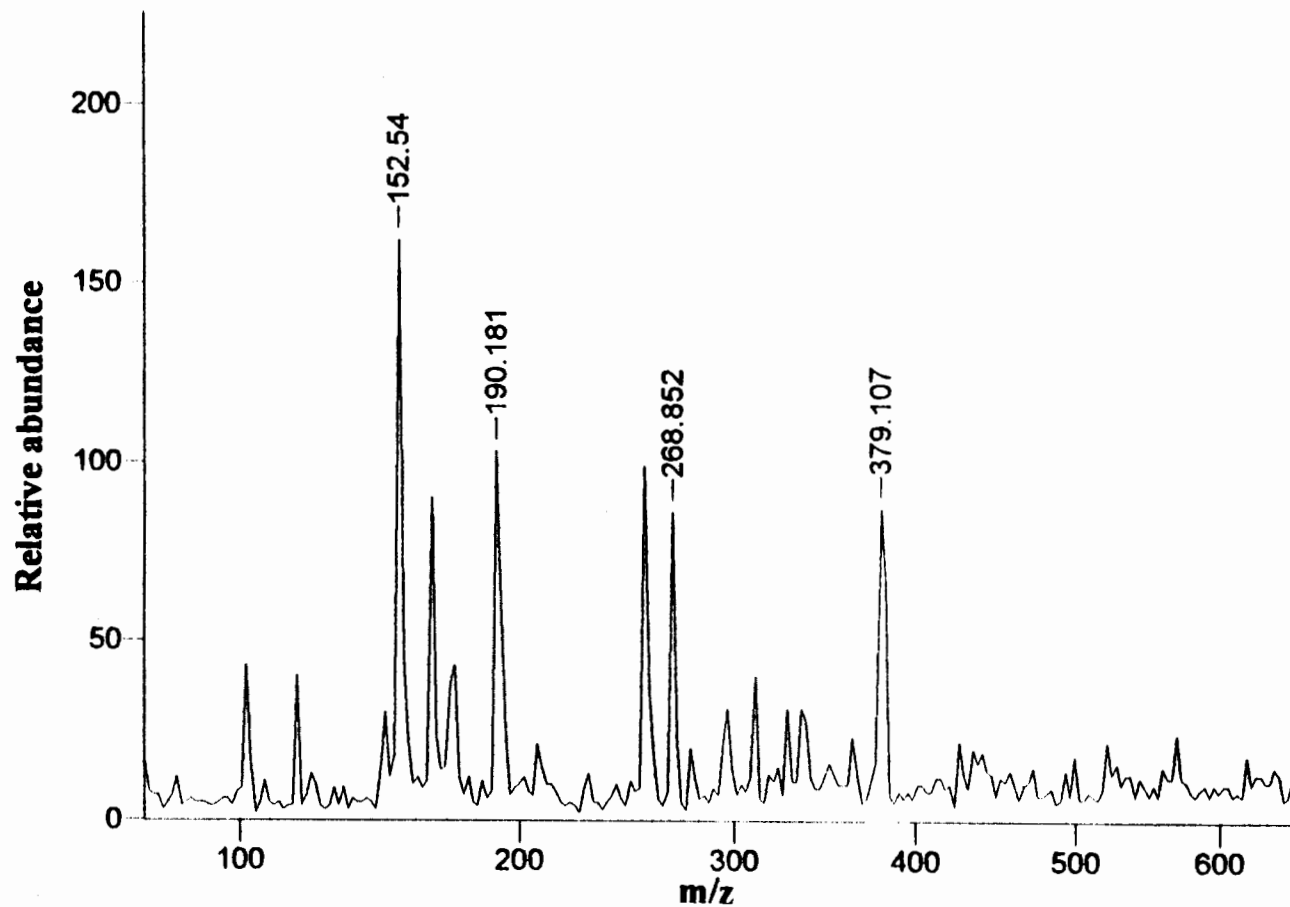


Fig. 16A MALDI MS spectrum of 2'-deoxyguanosine with 4HCC as matrix

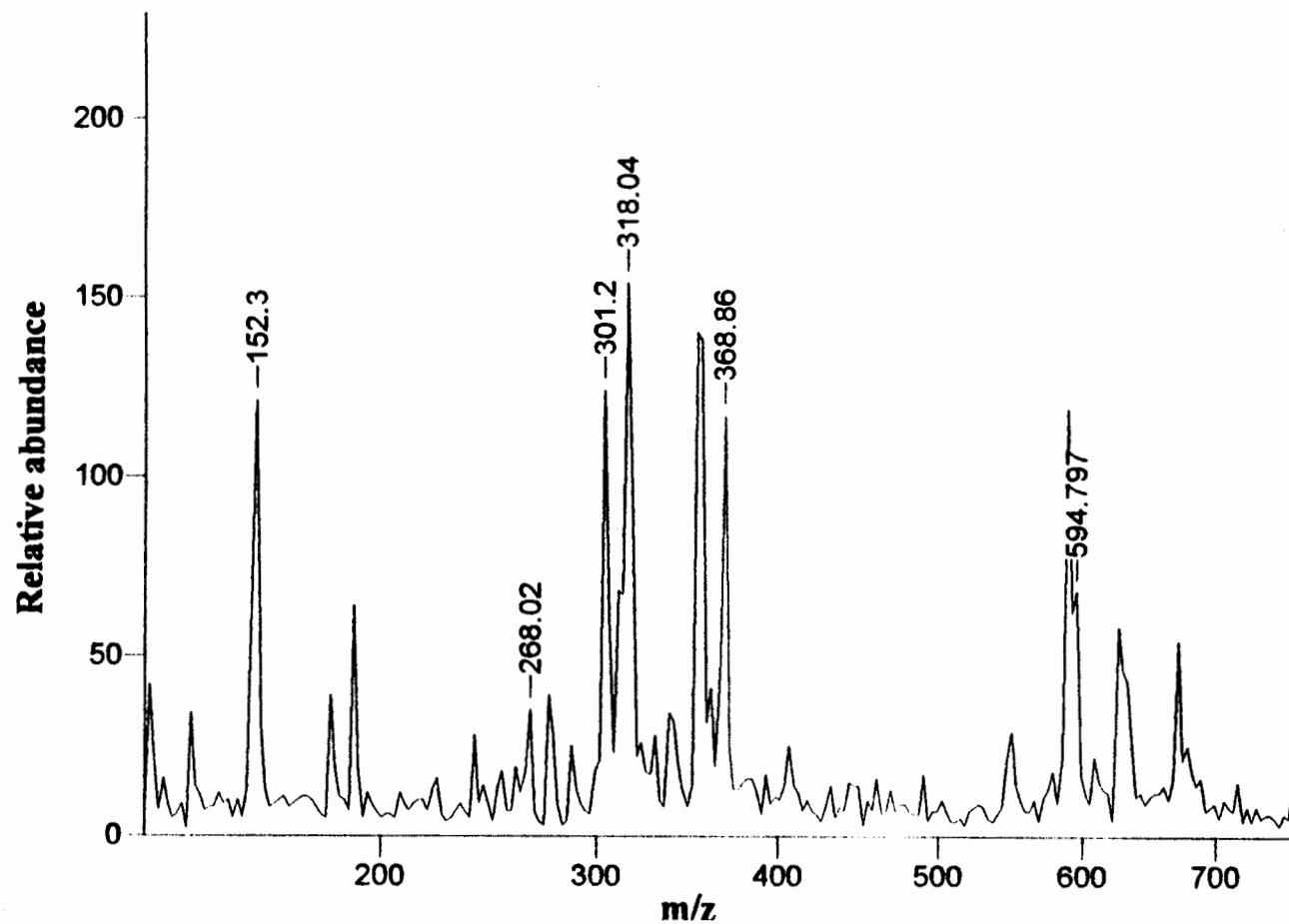


Fig. 16B MALDI MS spectrum of 2'-deoxyguanosine with BCC as matrix

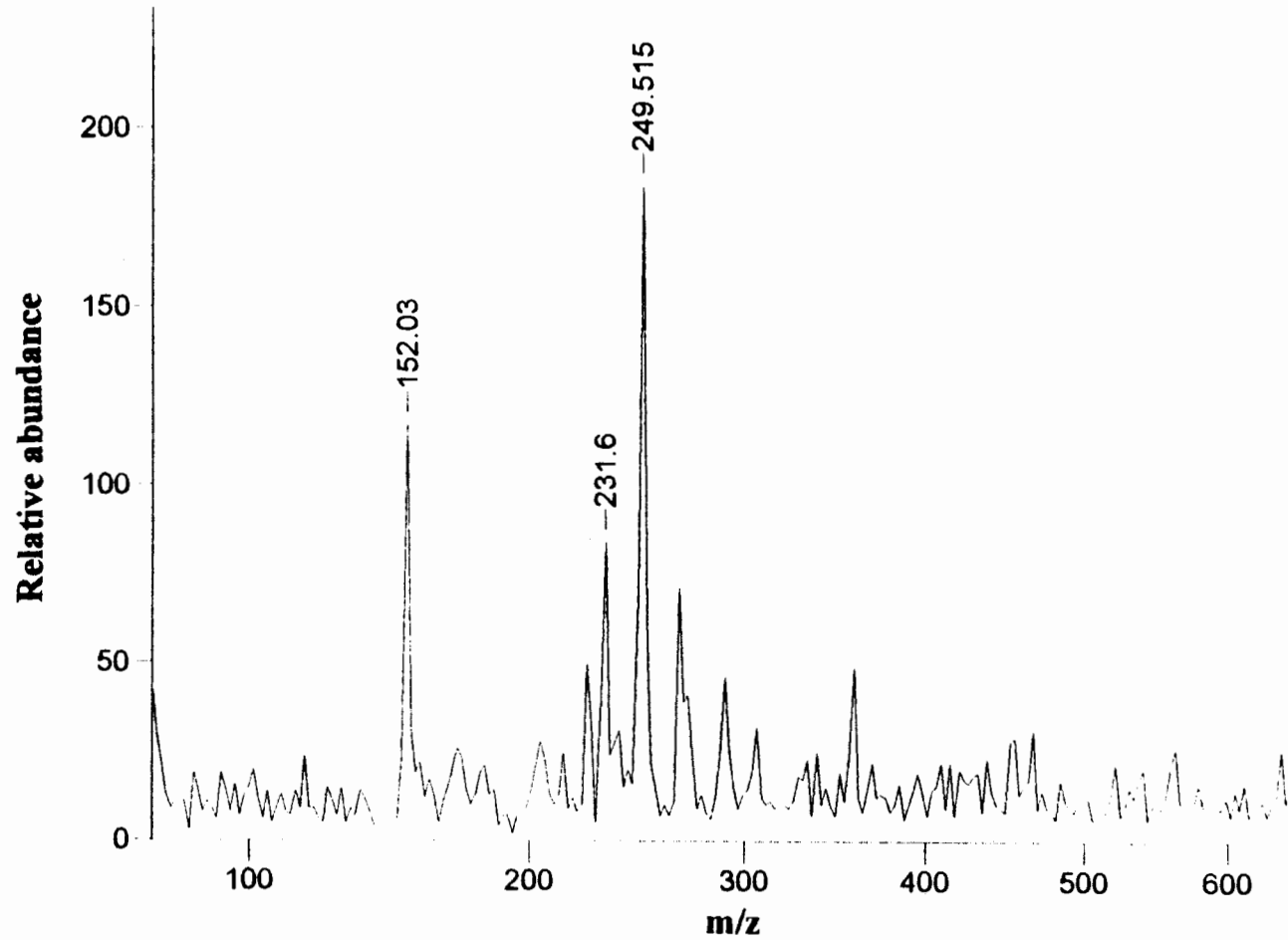


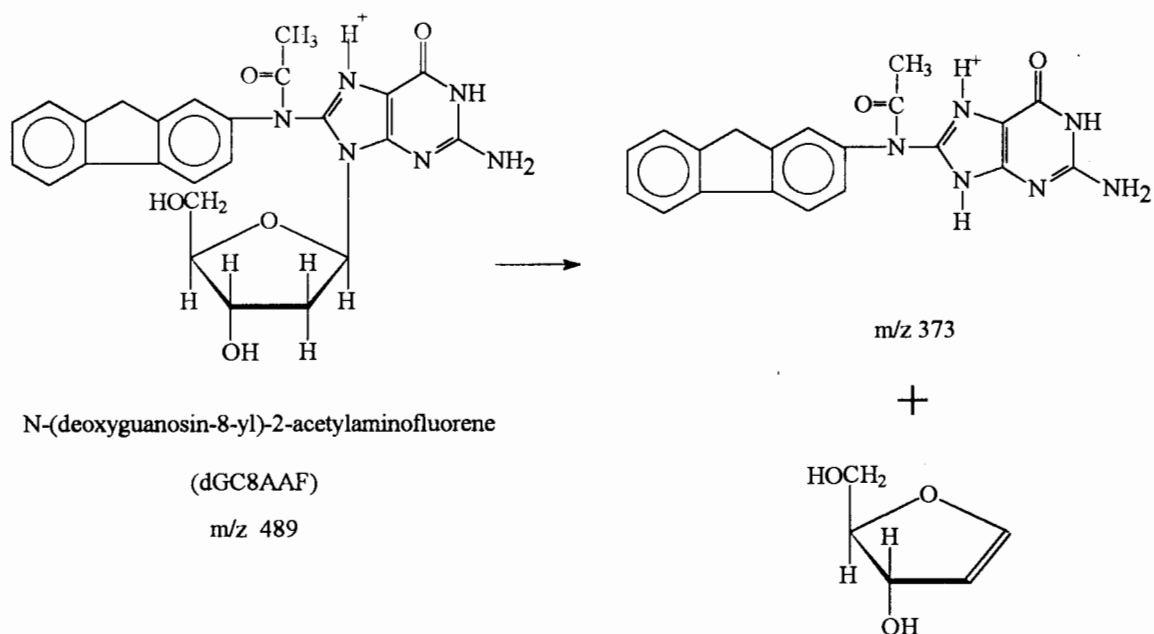
Fig. 16C MALDI MS spectrum of 2'-deoxyguanosine with PCC as matrix

all matrices. There was a peak at m/z 371 in PCC, therefore, PCC is not useful for this specific adduct. For 4HCC, there was a peak at m/z 379 $(2M+H)^+$, if adduct concentration is high enough, we observed m/z 373 adjacent to it. This ion at m/z 379 becomes insignificant at lower matrix concentrations. For 10 picomoles of adduct, we observed a little shoulder right next to this dimer ion, therefore, it is impossible to measure the resolution for 10 pmol of adduct in 4HCC. The limits of detection was found to be 10 picomole for saturated 4HCC and 5 picomole for PCC in a saturated solution.

The results of the matrix study are summarized in Table 2. In several instances, the molecular ion peak was obscured by the matrix.

B. Protein

We tested the utility of BCC and PCC with a small peptide, bovine insulin, to determine if these matrices were suitable for peptide analysis. Bovine insulin was chosen as a test compound because it is a common standard for MALDI-TOF MS calibration that normally gives strong signals in MALDI, and we assumed that a matrix would not be useful if it does not yield a strong response for insulin.



Scheme 4 dGC8AAF fragmentation pathway

Table 2

Matrices evaluation based on dG and dGC8AAF

Matrix	2'-deoxyguanosine		N-(deoxyguanosin-8-yl)-2-acetylaminofluorene	
	Resolution	LOD	Resolution	LOD
4HCCA	70.5	3.5 pmol	-	10 pmol
PCC	80	3.5 pmol	99	5 pmol
BCC	68	3.5 pmol	-	-

Note: Both resolution and limits of detection (LOD) were based on m/z 152 peak ; resolution was m/ m at full width of half maximum (FWHM)

Calibration was carried out using the peak for K^+ , the matrix dimer $(2M+H)^+$ at m/z 379, and the di- and monoprotonated peaks $(M+2H)^{2+}$ at m/z 2868 and $(M+H)^+$ m/z 5735 from bovine insulin.

The matrices used in this study were 4-hydroxy- α -cyanocinnamic acid (4HCC), ferulic acid (FA), caffeic acid (CA), sinapinic acid (SA), 3,5-dihydroxybenzoic acid (DHB), 4-benzyloxy- α -cyanocinnamic acid (BCC), and 4-phenyl- α -cyanocinnamic acid (PCC). All matrices surveyed yielded ions indicative of bovine insulin. Most matrices showed significant background up to about m/z 600 with laser power sufficient to produce peptide signals. The results of the study are summarized in Table 3.

Bovine insulin gave $(M+H)^+$ at m/z 5735 and $(M+2H)^+$ at m/z 2868 ions upon laser desorption from both PCC and BCC (Fig.18 A and B). Doubly charged peak $(M+2H)^{2+}$ was in lower intensity compared to single charged peak $(M+H)^+$, the dimer ion $(2M+H)^+$ of bovine insulin, was also observed at very low intensity and the peak width was very broad (Table 3). CA and FA (Fig. 19 A and B) gave better resolution for the singly charged peak, but the doubly charged peak showed little signal. Again, the dimer ion appeared in low relative abundance and was very broad. SA and DHB (Fig. 20 A and B) showed even better resolution than that of FA and CA for the singly charged peak, but there was Na^+ adduct peak in relative higher abundance right next to singly charged

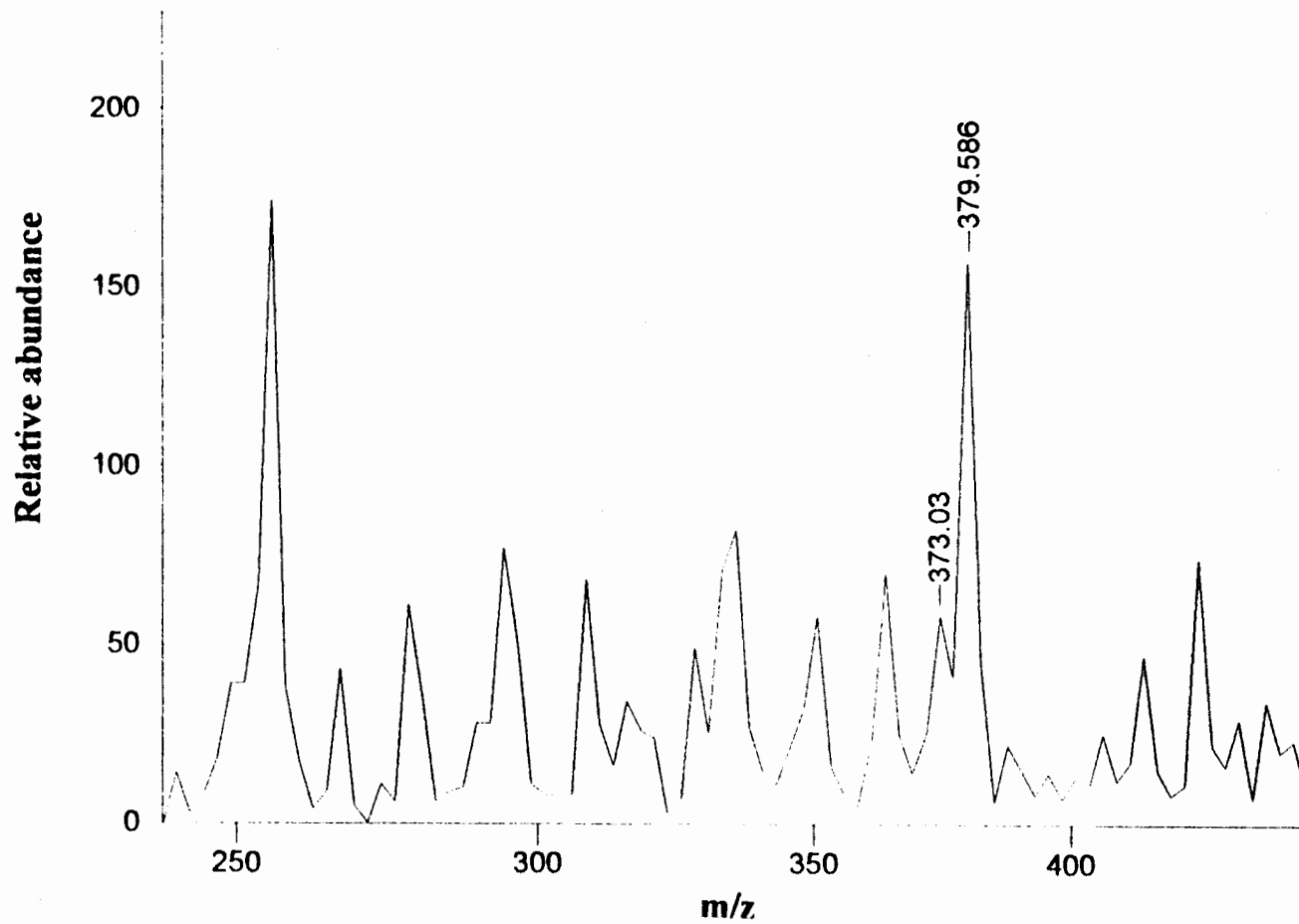


Fig. 17A MALDI MS spectrum of dGC8AAF with 4HCC as matrix

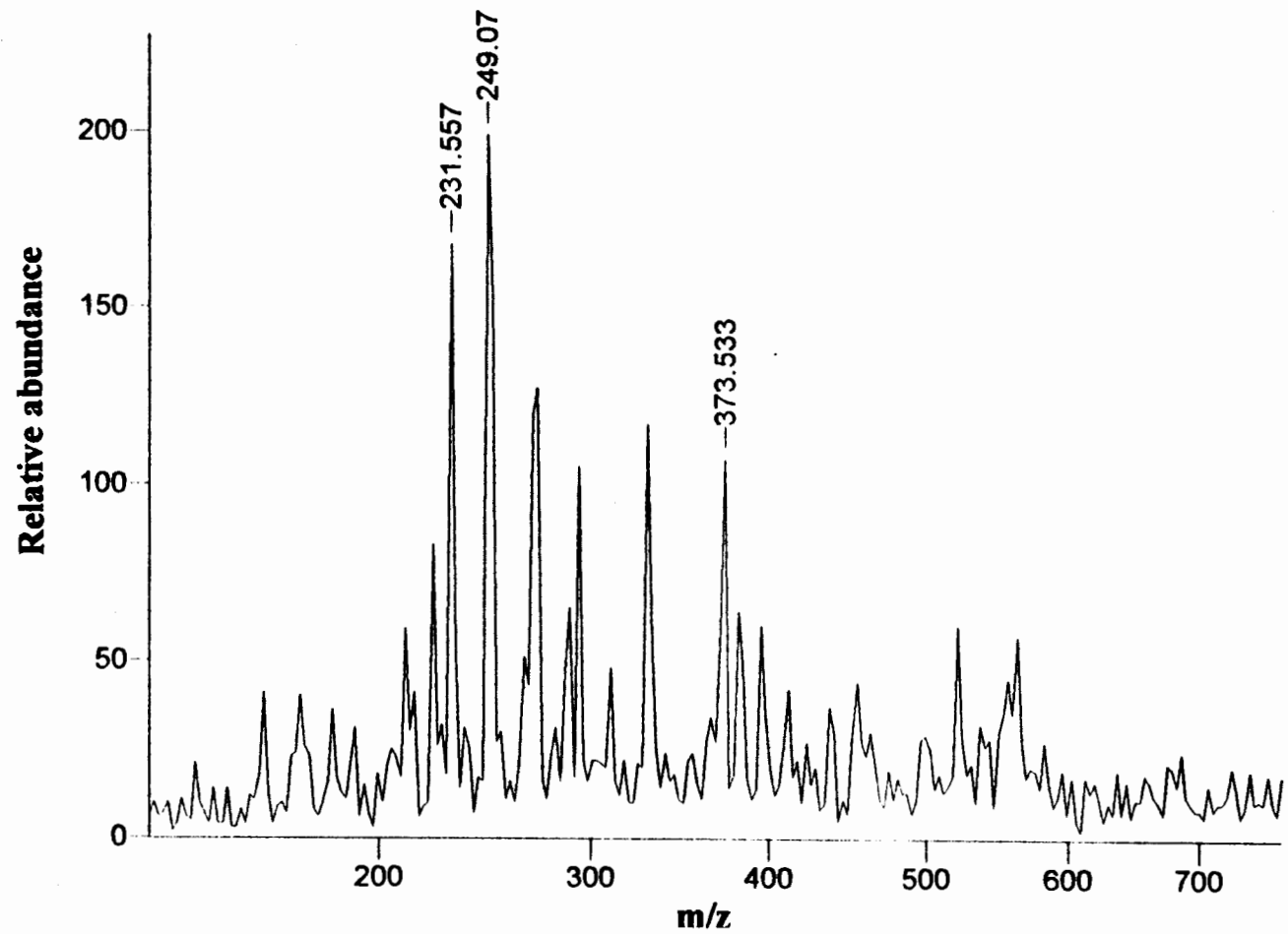


Fig. 17B MALDI MS spectrum of dGC8AAF with PCC as matrix

Table 3

Matrix evaluation based on bovine insulin

Matrix	Resolution	(M+H) ⁺	(M+H) ²⁺	(2M+H) ⁺
Caffeic Acid (CA)	41.5	+	+ low intensity	+
Ferulic Acid (FA)	35.0	+ Na ⁺ adduct	+ low intensity	+
Sinapinic Acid (SA)	59.0	+ Na ⁺ adduct	+ low intensity	+
4-Hydroxy- α -cyanocinnamic Acid (4HCC)	95.0	+	+ high intensity	+
4-Benzyloxy- α -cyanocinnamic Acid (BCC)	35.0	+	+ low intensity	+
4-Phenyl- α -cyanocinnamic Acid (PCC)	23.0	+	+ low intensity	+
2,5-Dihydroxy-benzoic acid (DHB)	50	+	+ low intensity	-

Note: Resolution was based on molecular ion (M+H)⁺ m/z 5735

+ detectable, - nondetectable

peak. The presence of adduct ions of high abundance adjacent to the $(M+H)^+$ peaks of proteins can interfere with accurate mass measurement. Doubly charged peaks and dimer peaks were formed with abundance for FA and CA. Both singly charged and doubly charged ions were observed at high relative abundance in 4HCC (Fig. 21). 4HCC efficiently promotes multiple protonation of the analyte and produces little matrix background. Of all matrices surveyed in this study we found that 4HCC was most generally useful based on resolution. However, DHB gave the least interference in low mass range. In addition to analysis of PAH-modified DNA adducts, PCC and BCC can be used as protein matrices as well, but they are not efficient as 4HCC.

In summarization, we synthesized two new matrices BCC and PCC. These two matrices are good for PAH-modified DNA adducts detection because of low detection limits and better resolution. In addition, they can be used as protein matrices.

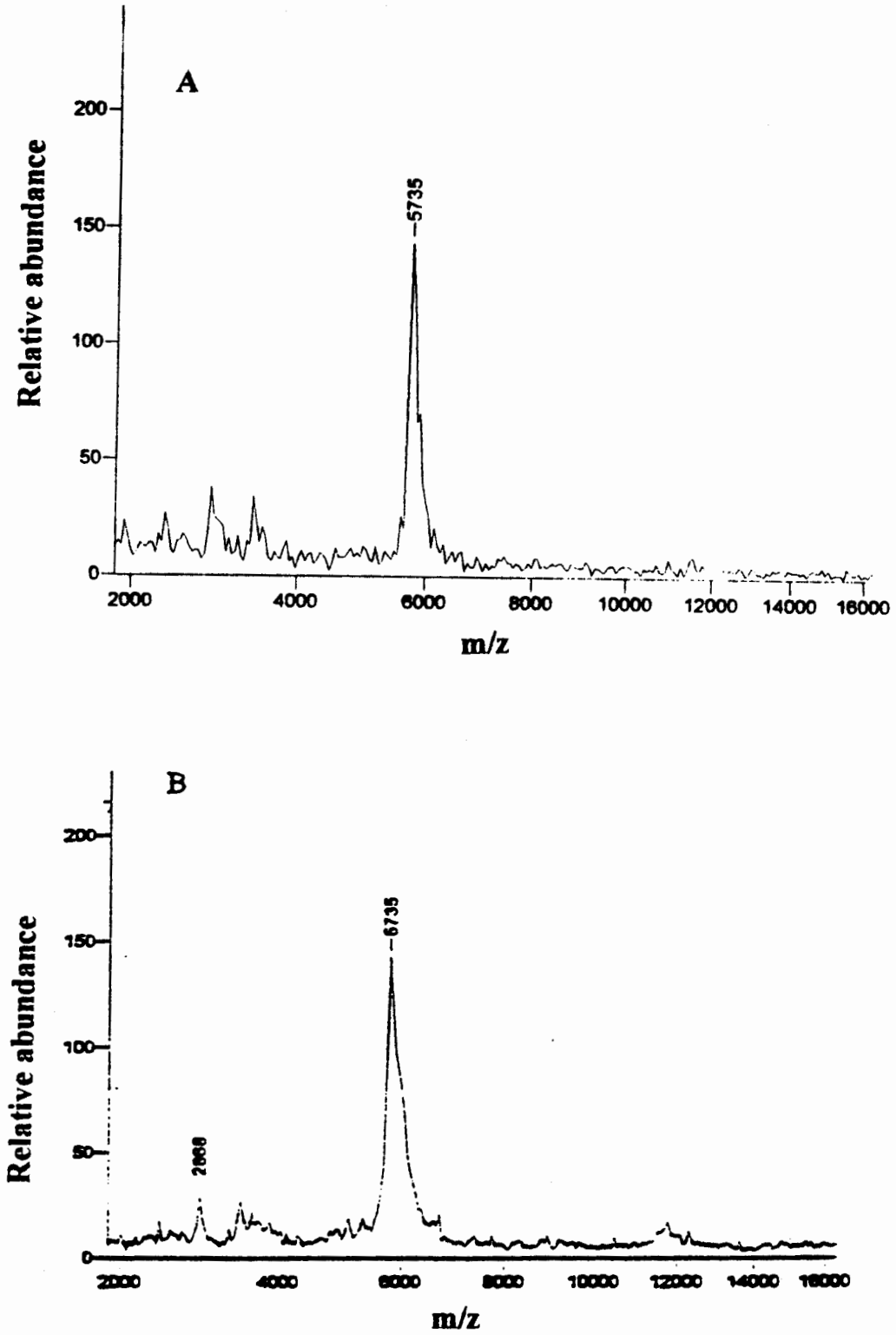


Fig. 18 MALDI MS spectra of bovine insulin in (A) BCC and (B) PCC matrices

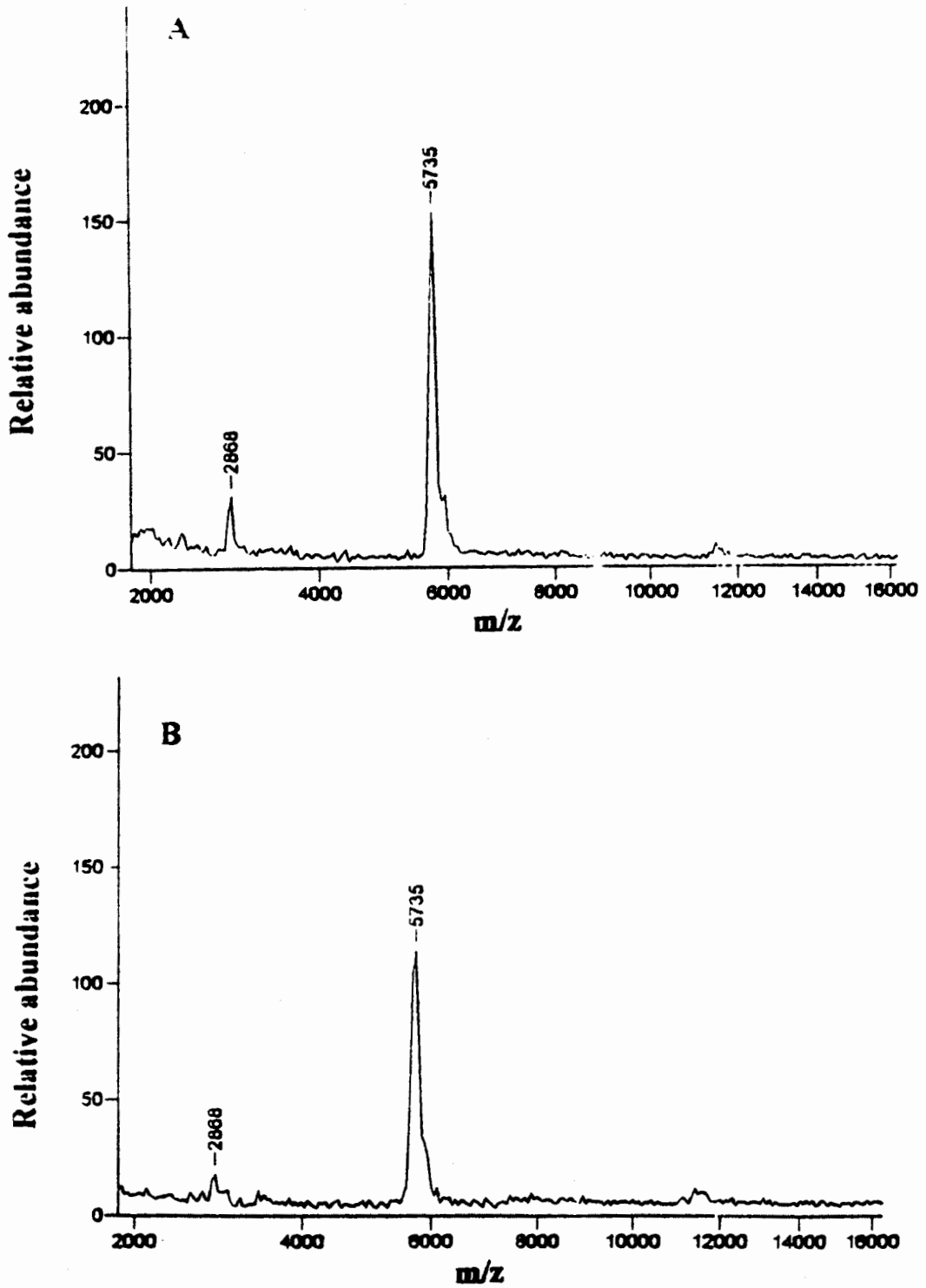


Fig. 19 MALDI MS spectra of bovine insulin in (A) CA and (B) FA matrices

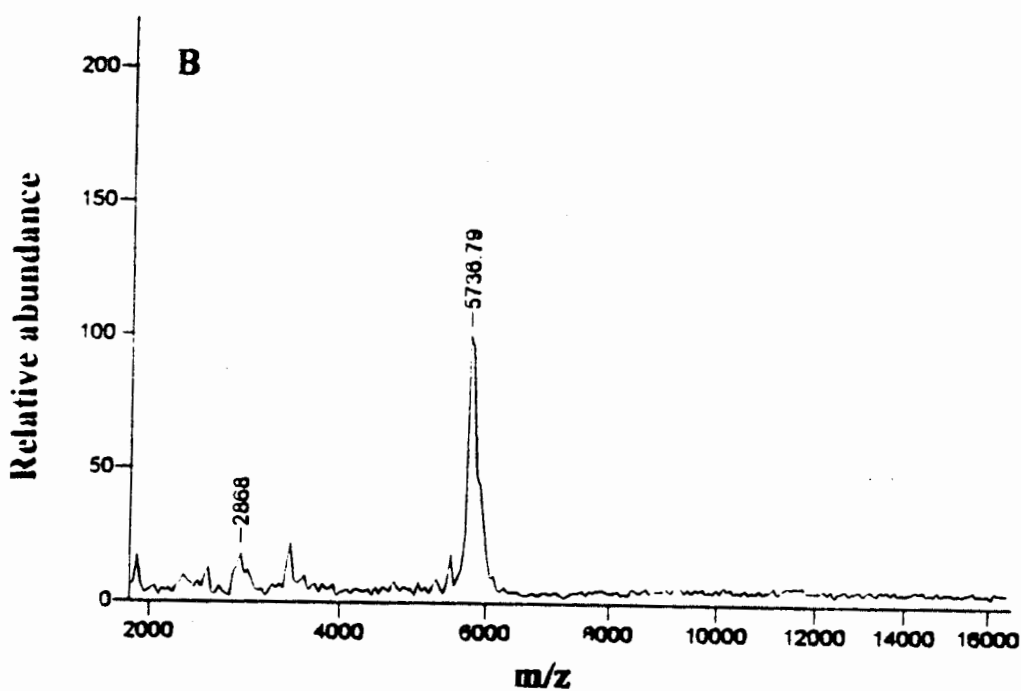
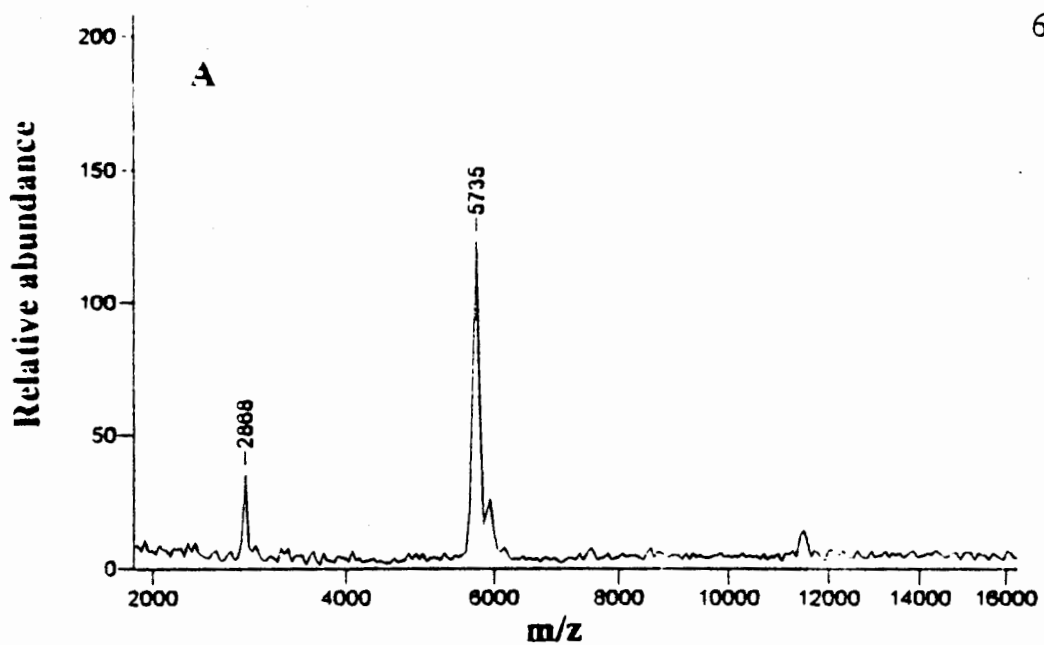


Fig. 20 MALDI MS spectra of bovine insulin in (A) SA
and (B) DHB matrices

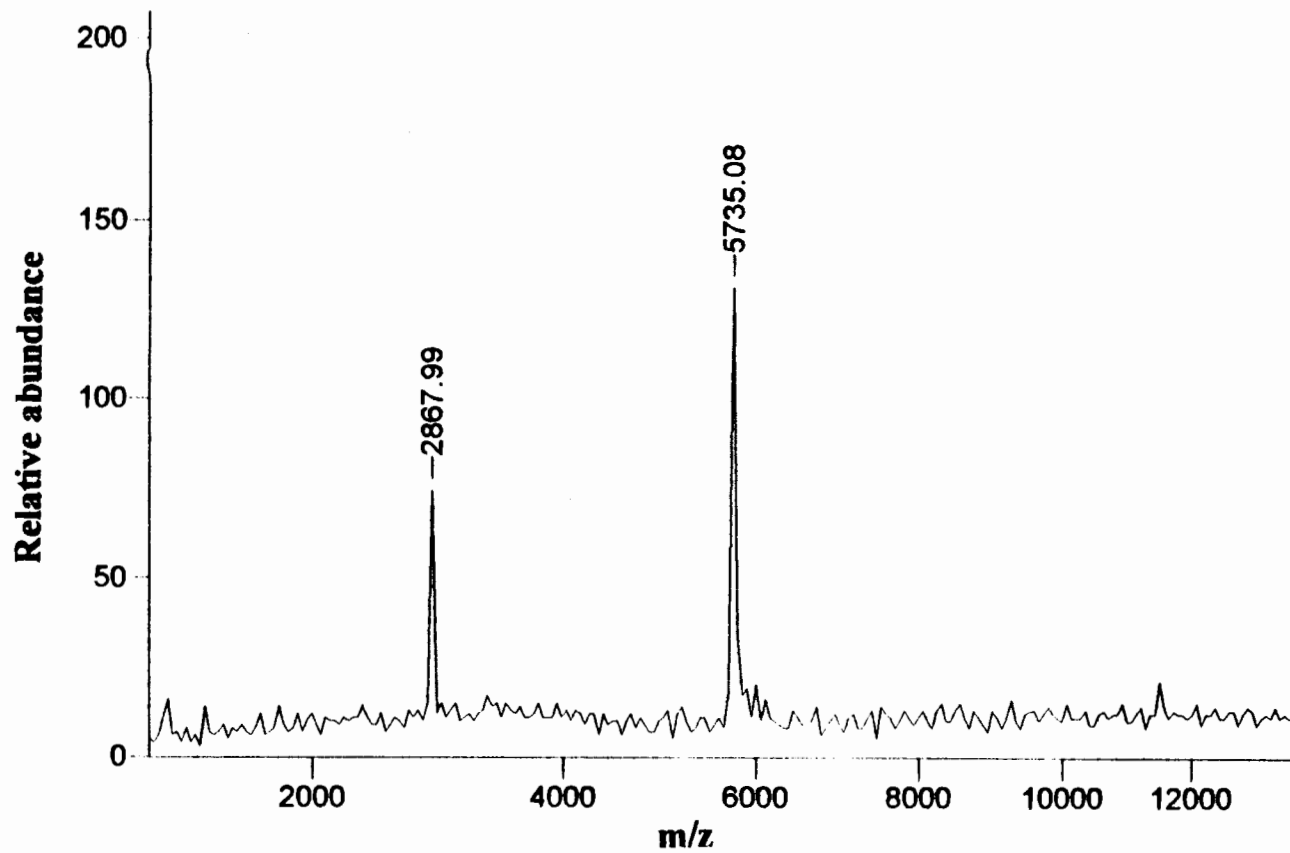


Fig. 21 MALDI MS spectrum of bovine insulin in a 4HCC matrix

CHAPTER IV

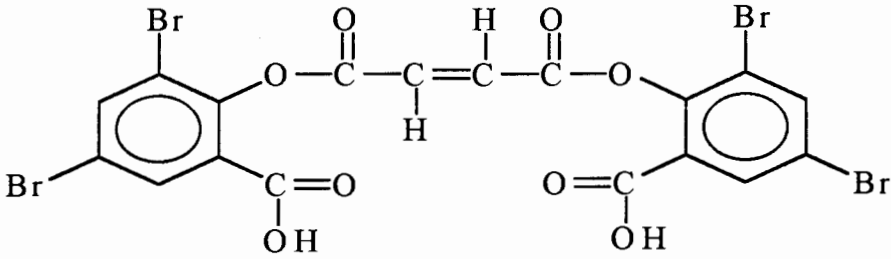
IDENTIFYING CROSS-LINKED HEMOGLOBIN BINDING SITES

Interest in developing potential blood substitutes stems from the limited blood supply available for emergency situations. Cross-linked hemoglobin as potential blood substitute has been studied for years (Winslow, 1992) because hemoglobin has a high capacity to bind oxygen and deliver it to tissues. However, hemoglobin, free in solution, can not be used as a blood substitute due to its dissociation from a $\alpha_2\beta_2$ tetramer to a $\alpha\beta$ dimer, which enables clearance from the bloodstream by the kidney. The oxygen affinity of the dimer is too large to allow tissues to absorb the oxygen. Chemically modifying hemoglobin is one way to overcome these problems. In order to develop more effective hemoglobin-based blood substitutes, we must understand the interrelationship between the possible changes that can be made in molecular structure during the modification, and how the changes affect the product's biological function such as oxygen binding affinity and inhibition of dissociation to dimers. Therefore, it is desirable to correlate the structure of a particular cross-linked hemoglobin with

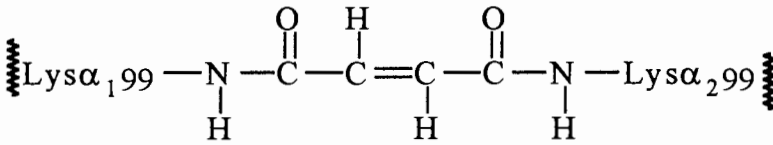
its oxygen affinity and stability with respect to dissociation.

The main sites for reaction on the hemoglobin molecule are located at N-terminal amino groups and the ϵ -amino groups of the lysine residues on the surface of the molecule. A few amino groups for crosslinking are available in the interior of the molecule such as lysine EF6(82) β in the 2,3-bisphosphoglycerate (2,3-BPG) pocket and lysine G6(99) α . There are forty reactive lysines (ϵ -amino groups), two α -chain amino-terminal α -amino groups, and two sulfhydryl groups (cysteine F9(93) β) in human hemoglobin. These groups can be accessed by various cross-linking reagents, so, there are many potential modification sites. Therefore, many different crosslinked products are possible and characterizing the structure of each product may be difficult.

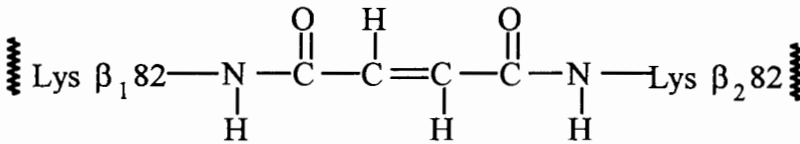
Bis(3,5-dibromosalicyl)fumarate (DBSF) is a reagent (scheme 6) that will cross-link human hemoglobin in the oxygenated (oxy) form. The more reaction product has more oxygen affinity than normal hemoglobin. The primary sites of reaction are lysine EF6(82) β_1 and lysine EF6(82) β_2 (Walder et al., 1980). However, when the same reaction is carried out under anaerobic conditions (deoxy), the product has reduced oxygen affinity. The primary sites of modification are lysine G6(99) α_1 and G6(99) α_2 (Chatterjee et al., 1986).



Bis (3,5-dibromosalicyl) fumarate (DBSF)



α 99 cross-linked hemoglobin



β 82 cross-linked hemoglobin

Scheme 6 DBSF cross-linking reagent and primary reaction products.

In the past, the reaction products of crosslinking reactions were characterized by X-ray crystallography (Fernandez, 1995). Molecular modeling is used to indicate those reaction conditions that would maximize the desired product, and thus simplifying the analytical characterization. However, peptide mass mapping by mass spectrometry can provide more detailed information about the number of modification sites. Peptide mass mapping is performed after cleavage of a protein (of known sequence) at selected sites by specific enzymes or chemical reagents. The calculated peptide mass can be compared to the experimentally observed peptide masses to identifying amino acid modification.

Matrix assisted laser desorption ionization mass spectrometry (MALDI MS) offers more accurate, sensitive detection of peptides, a combination of protein digestion and MALDI MS peptide mass mapping has been employed successfully in localizing the sites of chemical modification for a variety of proteins. Mass analyses offer a means of identifying or confirming position and a mass of particular chemical modification made to a protein through mass shift observed in comparing the mass spectra of digested native and modified versions of the protein.

The specific goal for this project is to develop a general methodology based on MALDI TOF MS for characterizing all possible products of a hemoglobin crosslinking reaction.

1. Identifying α 99XLHb and β 82XLHb cross-linked site by Trypsin Digestion

The first phase of this project was concerned with optimizing our MALDI mass-mapping strategy with well characterized crosslinked hemoglobins. Therefore, we examined the mass spectra of β 82XLHb and α 99XLHb before and after digestion with trypsin and cyanogen bromide (CNBr). In order to peptide mass mapping by MALDI MS, we have to cleave the hemoglobin into small pieces. The reason to use trypsin was due to its specific cleavage at C-terminal of lysine and arginine, since most of the cross-linked sites were believed to be on lysine. If a cross-link is located between amino groups of lysine, it will prevent trypsin hydrolysis at this lysine. Therefore, a tryptic fragment will be composed of two cross linked tryptic peptides (each containing an internal lysine). Location of the cross-linked site is achieved by comparing the mass of the cross-linked peptides with all the possible combination of tryptic peptides plus the mass of the linker reagent. The fragments obtained from cross-linked hemoglobin are larger than any tryptic fragments produced by tryptic Hb A, thus, facilitating the identification of the bound sites.

Hemoglobin A was used as one control experiment. MALDI MS analysis of tryptic digest of Hb A did not show all the expected tryptic fragments (Table 4, 5, 6, 7 listed all the tryptic pieces and corresponding mass value from α and β

chain respectively). Fig. 22 is a spectrum of tryptic digested hemoglobin. Since Hb A contains two α chains and two β chains, with total molecular weight around 64,000 Da, it was not surprising that we did not cover all expected the peaks, but obtained the multiplicity of fragments produced. There were reports that coverage of the peptide mapping in a MALDI MS mass map generally decrease with increasing molecular weight of the protein (Juhasz et al., 1993 and Billeci et al., 1993), therefore, successful application of our strategy will require a partial separation of complicated peptide mixtures.

For β 82XLHb, with a fumarate cross-link between K₈₂- β 1 and K₈₂- β 2 of HbA, we expect to see two pieces composed of V₆₇-K₉₅ ($[M+H]^+_{\text{calc}} = 3073.5$) linked by fumarate (mass 82) which causes a mass shift to $(M+H)^+_{\text{calc}} = (3073.5 \times 2 + 82 + 1) = 6230$. For α 99XLHb, another fumarate cross-linked Hb, the bonding site is believed to be between K₉₉- α 1 and K₉₉- α 2, we expected to two tryptic peptide V₉₃-K₁₂₇ ($[M+H]^+_{\text{calc}} = 3770.5$) linked by fumarate cause mass shift to $(M+H)^+_{\text{calc}} = (3770.5 \times 2 + 82 + 1) = 7624$. Under ideal conditions, we expect the fragments $(M+H)^+_{\text{calc}} = 1670.9$ for V₆₇-K₈₂, and $(M+H)^+_{\text{calc}} = 1422.6$ for G₈₃-K₉₅ for β 82 XLHb to be absent and a new fragment at m/z 6230 appear. For α 99XLHb, we expect the two fragments at $(M+H)^+_{\text{calc}} = 819.0$ for V₉₃-K₉₉ and $(M+H)^+_{\text{calc}} = 2969.5$ for L₁₀₀-K₁₂₇ to be absent, and a new fragment at m/z

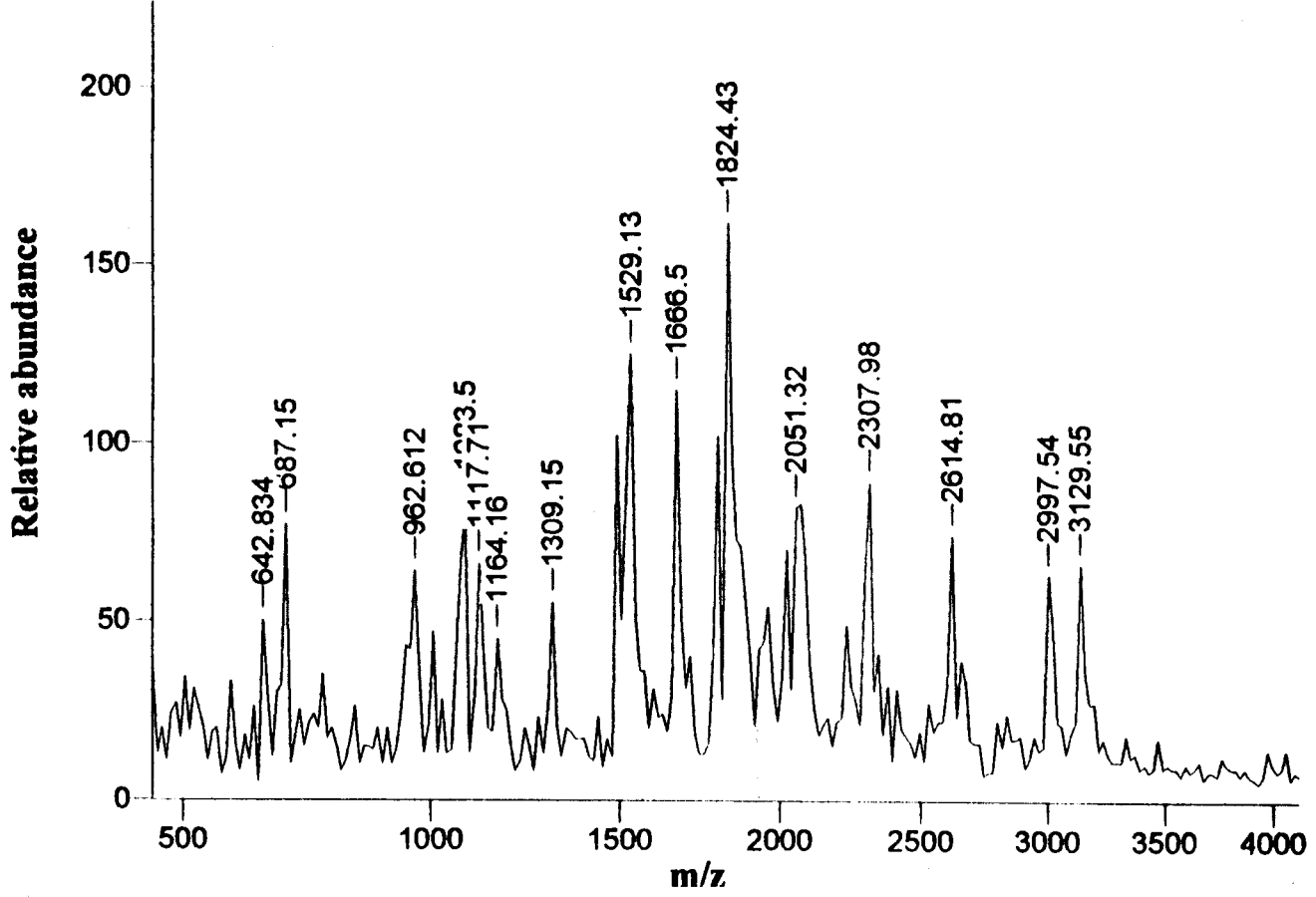


Fig. 22 MALDI MS of tryptic digest of hemoglobin

7624 to appear in the mass spectrum.

By comparing tryptic digest of XLHb β 82 MALDI MS spectrum with Hb A, we were not able to generate useful information, because the expected peak m/z 6230 was not observed. As for tryptic digest of α 99XLHb, we did observe a peak in the MS spectrum (Fig. 23), m/z 7623 consistent with what we calculated value (m/z 7624) for this cross-linked hemoglobin. However, peak abundance was near the limit of detection. The reason we did not observe fragment at m/z 6230 for β 82XLHb could be different ionized process for this fragment or detector saturation. However, we observed some peaks around 3000~4000 amu for both XLHb α 99 and XLHb β 82, which not observed in the mass spectra of the Hb A. Fig. 24 and 25 are mass spectra of the β 82XLHb and the α 99XLHb tryptic digest. There were three peaks in the β 82XLHb, at m/z 3016, 3129, and 3303. The peak at m/z 3129 is likely from the K₆₆-R₁₀₄ fragment of the β chain plus the linker, and the peak at m/z 3303 is likely from the K₆₂-R₁₀₄ fragment of the β chain plus the linker. We observed a cluster of peaks at m/z 3896, m/z 4178, and m/z 4493 in mass spectra of the α 99XLHb tryptic digest. The peaks at m/z 3896, and m/z 4178 correspond to the V₉₃-K₁₂₇ and V₉₁-K₁₂₇ fragments of α chain respectively, each bound to a fumarate crosslink individually. Since we observed the fragment for the cross-linked hemoglobin in MALDI analysis, those

fragments m/z around 3000~4000 were likely due to the uncompleted crosslinking reaction.

Table 4
Hb β Chain tryptic digest fragments

position in sequence	Amino acid residues
1-8	VHLTPEEK
9-17	SAVTALWGK
18-30	VNVDEVGGEALGR
31-40	LLVVYPWTQR
41-59	FFESFGDLSTPDAVMGNPK
60-61	VK
62-65	AHGK
66	K
67-82	VLGAFSDGLAHLNLK
83-95	GTFATLSELHCDK
96-104	LHVDPENFR
105-120	LLGNVLCVLAHHFGK
121-132	EFTPPVQAAYQK
133-144	VVAGVANALAHK
145-146	Y

Table 5

Hb α Chain tryptic digest fragments

position in Sequence	Amino Acid Residues
1-7	VLSPAAK
8-11	TNVK
12-16	AAWGK
17-31	VGAHAGEYGAEALER
32-40	MFLSFPTTK
41-56	TYFPHFDSLHGSAEVK
57-60	GHGK
61	K
62-90	VADALTNAVAHVDDMPNALSALSDDLHAHK
91-92	LR
93-99	VDPVNFK
100-127	LLSHCLLVTLAAHLPAEFTPAVHASLDK
128-139	FLASVSTVLTTSK
140-141	YR

Table 6Hb α chain tryptic digest fragments corresponding mass value

Position in sequence	(M+H) ⁺	Position in sequence	(M+H) ⁺
1-7	729.9	62-90	2998.4
8-11	462.0	91-92	288.0
12-16	532.6	93-99	819.0
17-31	1530.6	100-127	2969.5
32-40	1072.3	128-139	1253.5
41-56	1835.0	140-141	338.0
57-60	381.0		

Table 7Hb β chain tryptic digest fragments corresponding mass value

Position in sequence	(M+H) ⁺	Position in sequence	(M+H) ⁺
1-8	952.1	67-82	1670.9
9-17	933.1	83-95	1422.6
18-30	1315.4	96-104	1127.2
31-40	1275.5	105-120	1721.1
41-59	2060.3	121-132	1379.6
60-61	245.0	133-144	1150.4
62-65	421.0	145-146	318.0

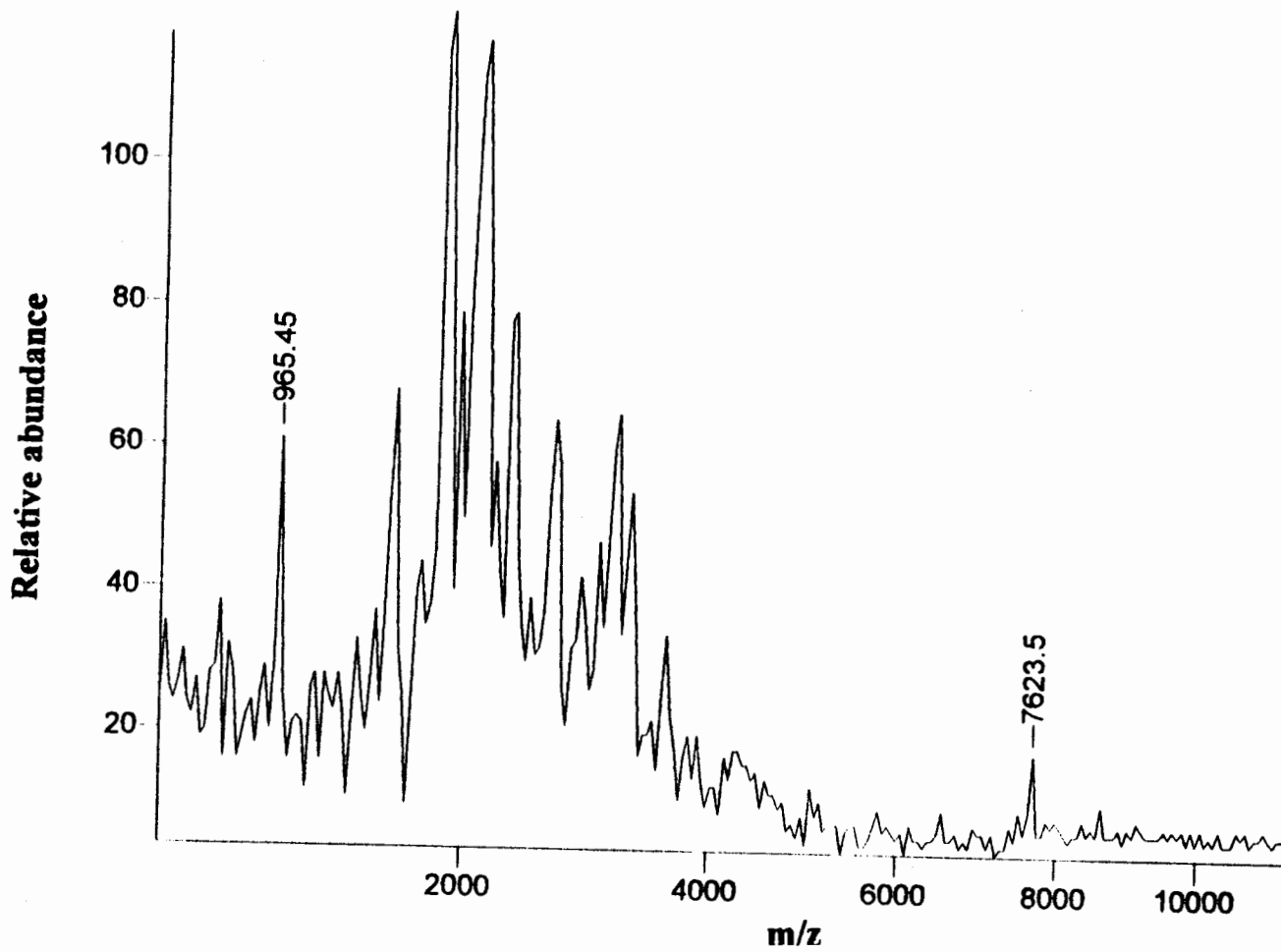


Fig. 23 MALDI MS spectrum of tryptic digest of α 99XLHb

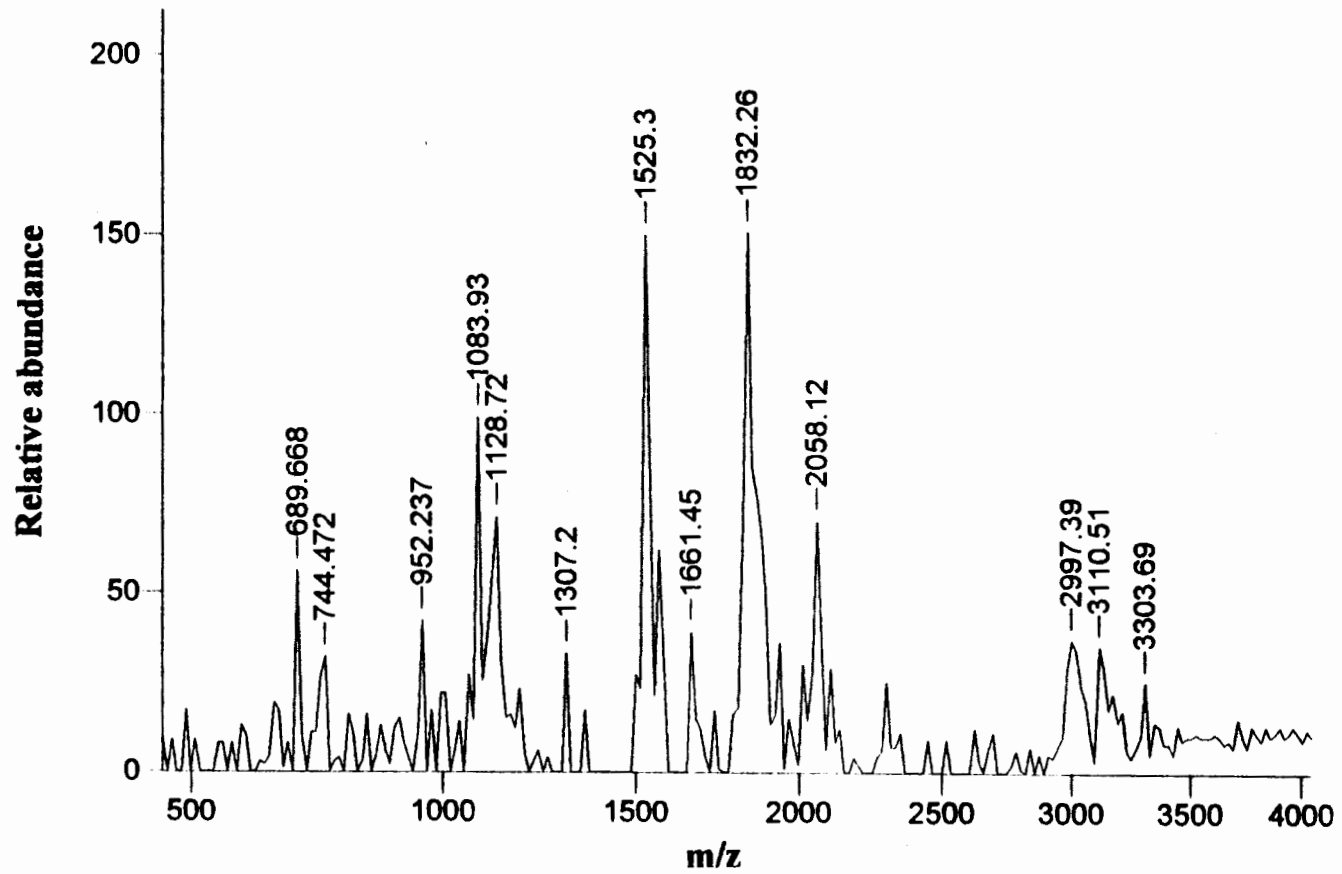


Fig. 24 MALDI MS spectrum of tryptic digest of β 82XLHb

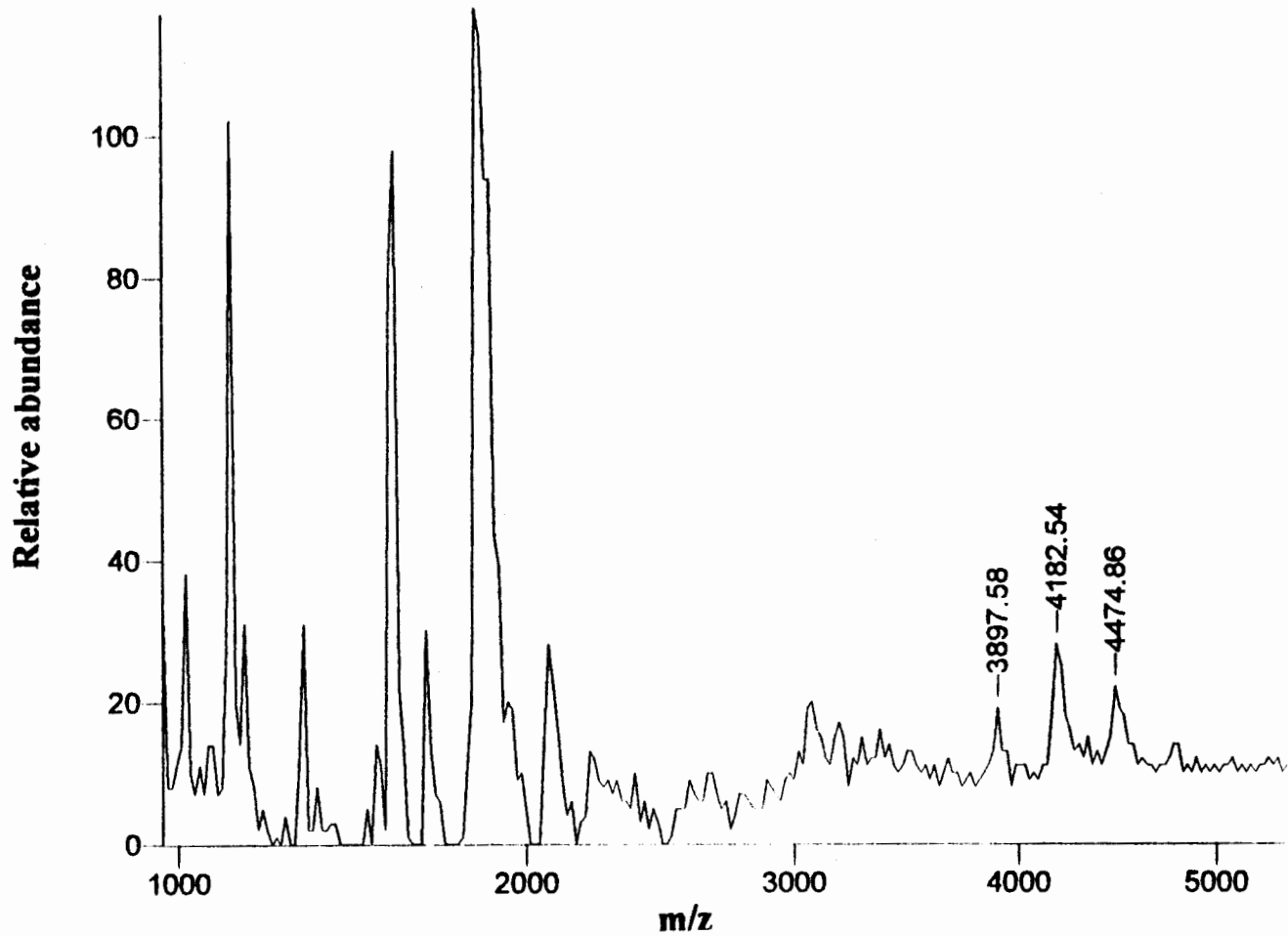


Fig. 25 MALDI MS spectrum of tryptic digest of α 99XLHb

Because unlinked HbA tryptic peptide mass mapping only gave small peptides, i.e. $m/z < 3000$, we thought that microcon filter with a mass cut off of 3000 amu would be useful for isolating cross-linked tryptic fragments. However, since only those fragments in m/z 3000- m/z 4000 region were observed, the attempt failed.

2. MALDI mass mapping of cross-linked hemoglobin with cyanogen bromide digestion

The mass spectra of the tryptic digests did not yield significant abundance of the cross-linked tryptic fragments, therefore, we opted for a digestion process that would yield simpler spectra.

Cyanogen bromide, in the presence of acid, cleaves the proteins at the C-terminus of each methionine. Since proteins usually contain only a few methionine residues, cyanogen bromide digestion produces only a few peptides, making mass map spectra easier to interpret than the digest produced by trypsin.

The cyanogen bromide digest fragments expected for unlinked human hemoglobin are listed in Table 8.

Table 8

Hemoglobin A CNBr digest fragments corresponding mass values

α Chain		β Chain	
Position in sequence	(M+H) ⁺	Position in sequence	(M+H) ⁺
1-32	3264.7	1-55	6000.8
33-76	4724.3	56-146	9806.4
77-141	7032.3		

Screening of the unlinked Hb A and cross-linked Hb A cyanogen bromide digest fragments should provide insight into the primary cross-linked sites. The cross-linked sites are located either at β chain of lysine 82 or α chain of lysine 99. Therefore, for β 82XLHb we expect to see a fragment m/z 19694 and the fragment at m/z 9806 at reduced abundance compared to the CNBr digest of hemoglobin A. In the spectra of α 99XLHb CNBr digest, we expect to observe a peptide fragment at m/z 14135. We expect the fragment at m/z 7026 to be weak or not observed at all in the spectra of the α 99XLHb CNBr digest. The MALDI mass spectra of the CNBr digests of the α 99XLHb, β 82XLHb and Hb A are given in Fig. 26-28 respectively. The spectrum of hemoglobin A yield all five

expected fragments. The MALDI spectra of the α 99XLHb shows four fragments. The fragment at m/z 7026 was not observed as we expected, however, the cross-linked fragment at m/z 14135 was absent as well. The β 82XLHb CNBr digest spectra gave four fragments as well. The fragment at m/z 9806 was not observed, suggesting that this fragment was cross-linked. A weak signal corresponding to the cross-linked fragment was observed at m/z 19694. Since cyanogen bromide digest only cleave on C-terminal of methionine, and one CNBr of fragment contains many lysines, we can not know exactly which of these lysines are bound, therefore, it can not provide exact information of the binding site.

The CNBr digest of both cross-linked HbA (either at α -99 lysine or β -82 lysine) produce cross-linked fragments whose mass value greater than 10,000 amu. So we sought to isolate these fragments with a centricon mass 10,000 cut-off filter, then to do tryptic digestion and MALDI MS analyses. The MALDI MS analysis of the tryptic fragments should cover the whole digest of the crosslinked CNBr fragments unlike the tryptic digest of the entire cross-linked HbA. Therefore, we opted to evaluate the strategy delineated in the scheme 6 to characterize the cross-linked products.

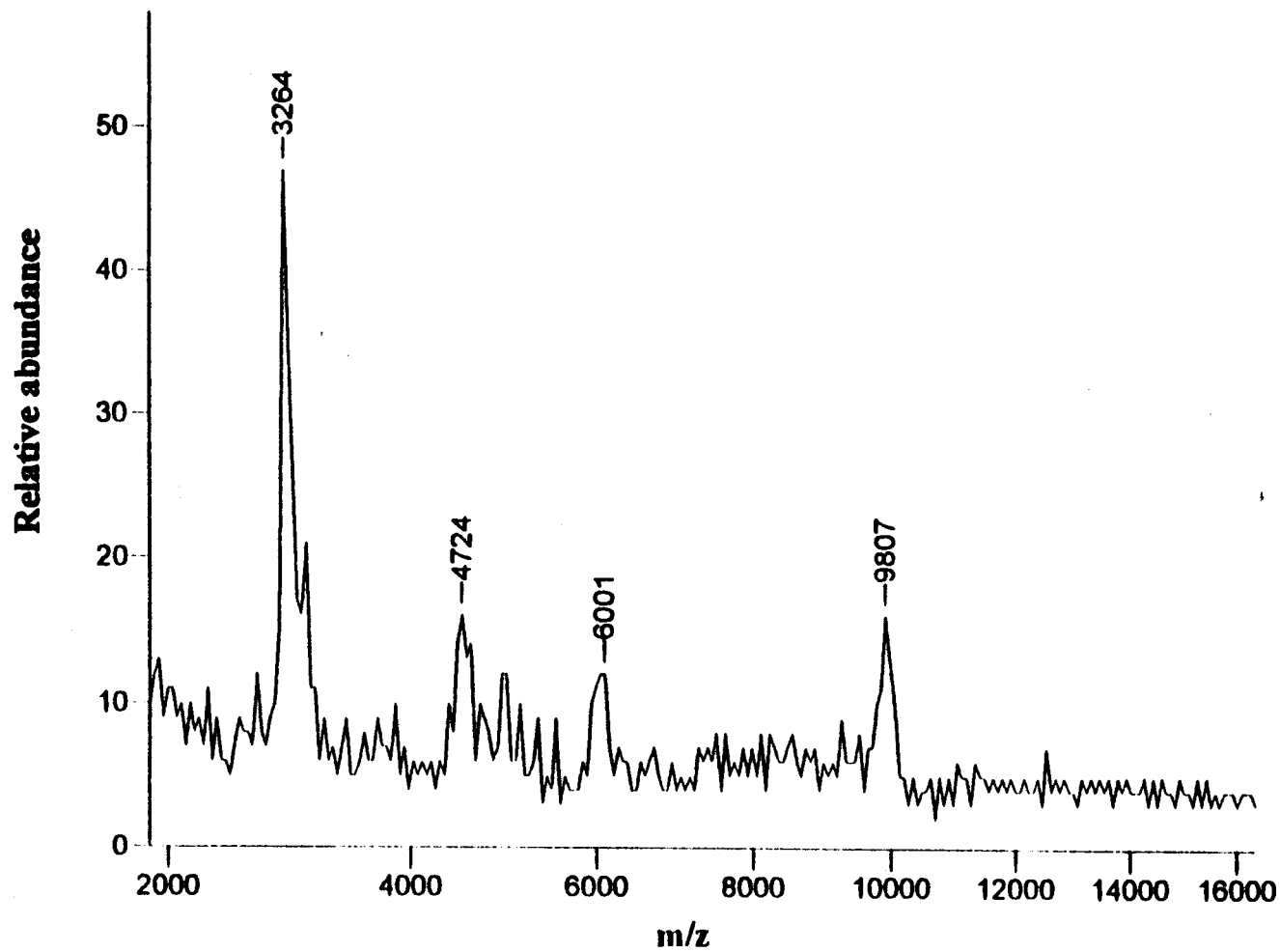


Fig. 26 MALDI MS spectrum of CNBr digest of α 99XLIb

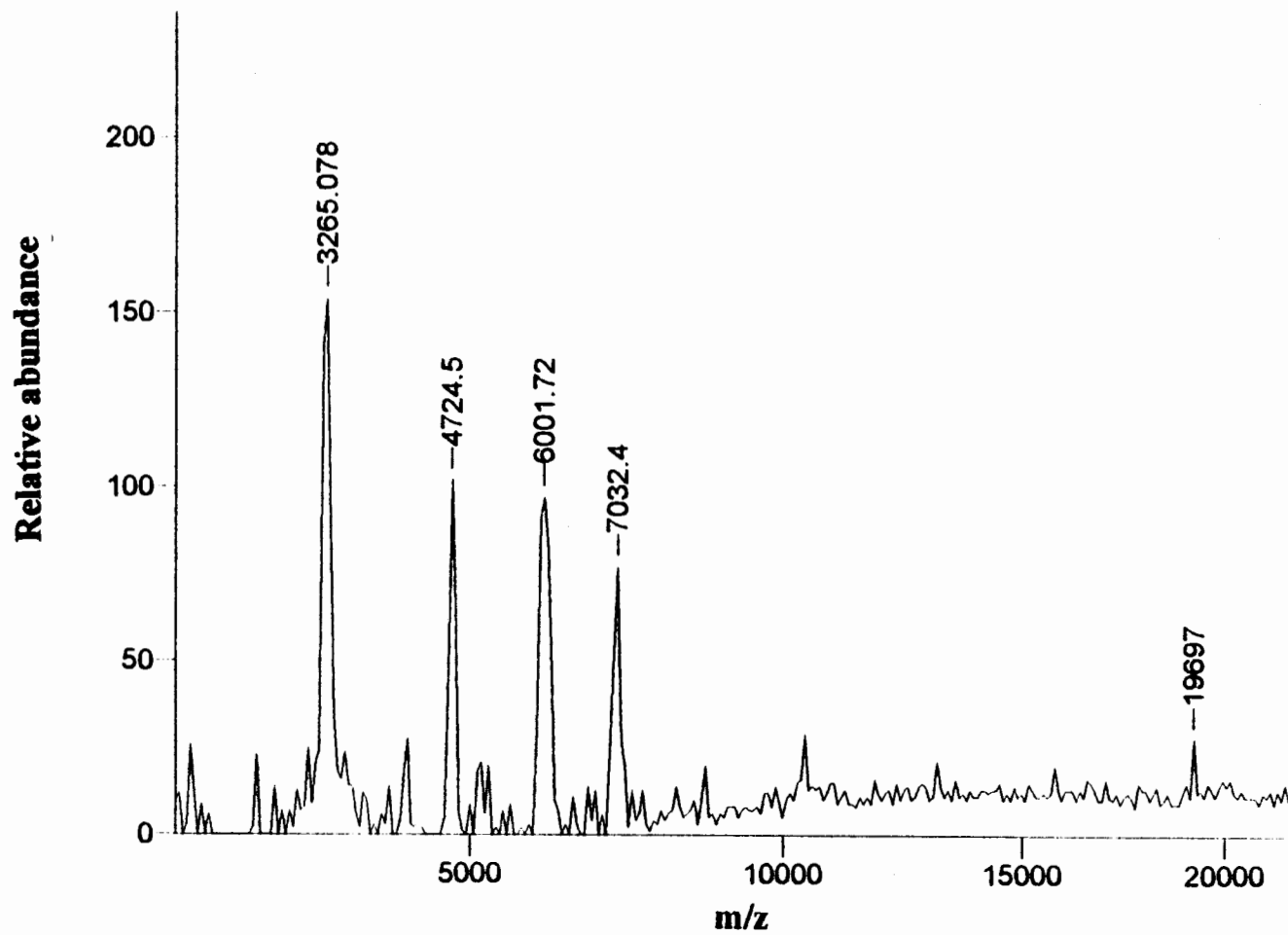


Fig. 27 MALDI MS spectrum of CNBr digest of β 2XLHb

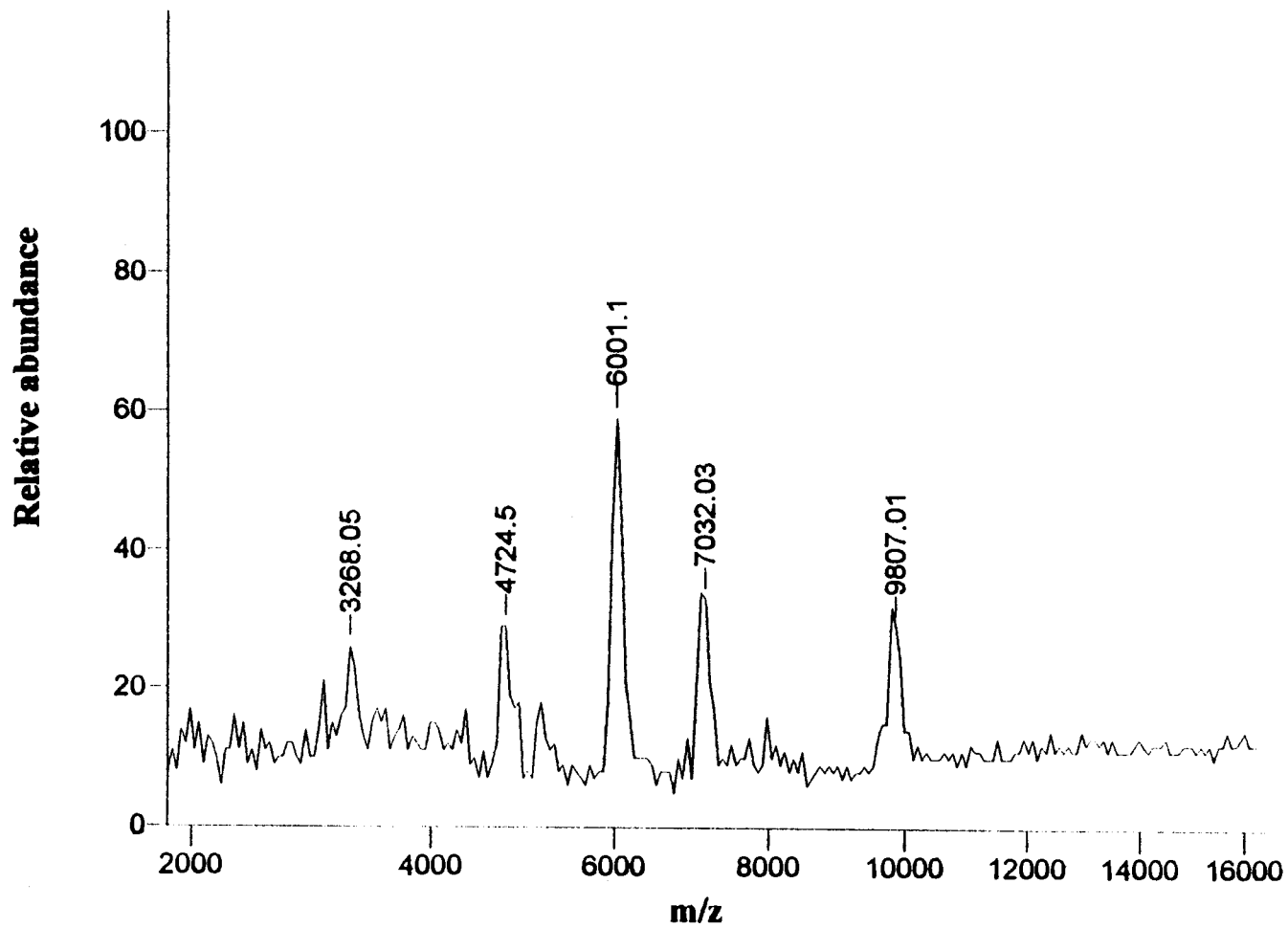
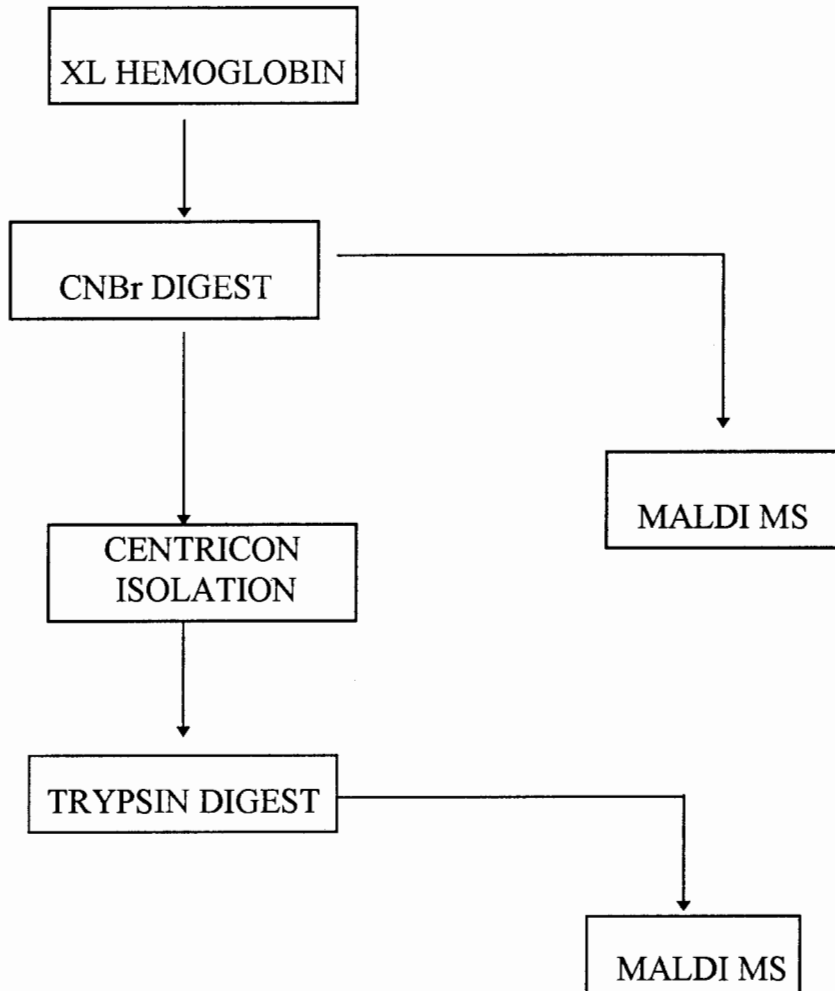


Fig. 28 MALDI MS spectrum of CNBr digest of hemoglobin

STRATEGY



Scheme 6 Strategy for identifying cross-linked site

The MALDI mass spectrum shown in Fig. 29 was recorded from a tryptic digest of cyanogen bromide fragments of cross-linked human hemoglobin by

fumarate at lysine 99 position in the α chain, yield only a suggestion of the expected cross-linked tryptic fragment at m/z 7623. The tryptic peptide V_{93} - K_{127} of the α chain of Hb A has a calculated molecular weight of 3770.5 and one internal lysine residue at position 99. A fumarate cross-link (causes a mass shift of 82 amu) between K_{99} - $\alpha 1$ and K_{99} - $\alpha 2$ of Hb A tetramer would be expected to produce a MALDI MS ion of the type $(M+H)^+_{\text{calcl}} = 3770.5 \times 2 + 82 + 1 = 7632$. An observed signal at $m/z = 7623$ provides experimental evidence for a fumarate K_{99} - $\alpha 1$ and K_{99} - $\alpha 2$ cross-link.

A MALDI spectrum of the tryptic digest of the crosslinked CNBr fragment from $\beta 82$ XLHb is given in Fig. 30. The tryptic peptide V_{67} - K_{95} of the β chain of HbA has a calculated molecular weight of 3073.5 and one internal lysine residue at position 82. A fumarate cross-link between K_{82} - $\beta 1$ and K_{82} - $\beta 2$ of the HbA tetramer would be expected to produce a MALDI MS ion of the type $(M+H)^+ = (3073.5 \times 2 + 86 + 1) = 6223$. The signal at m/z 6224 provides experimental evidence. For a fumarate K_{82} - $\beta 1$ and K_{82} - $\beta 2$ cross-link. Further evidence for localization of this chemical modification for the fragment observed at m/z 7337.0. In this case, the partial tryptic peptide V_{67} - R_{104} of the β chain of HbA (Zaluzec et al., 1995), having a calculated molecular weight of 4182.0, produced MALDI MS ions of the type $(M+H)^+_{\text{cacl}} = [(3073.5 + 4182.7) + 82 + 1] =$

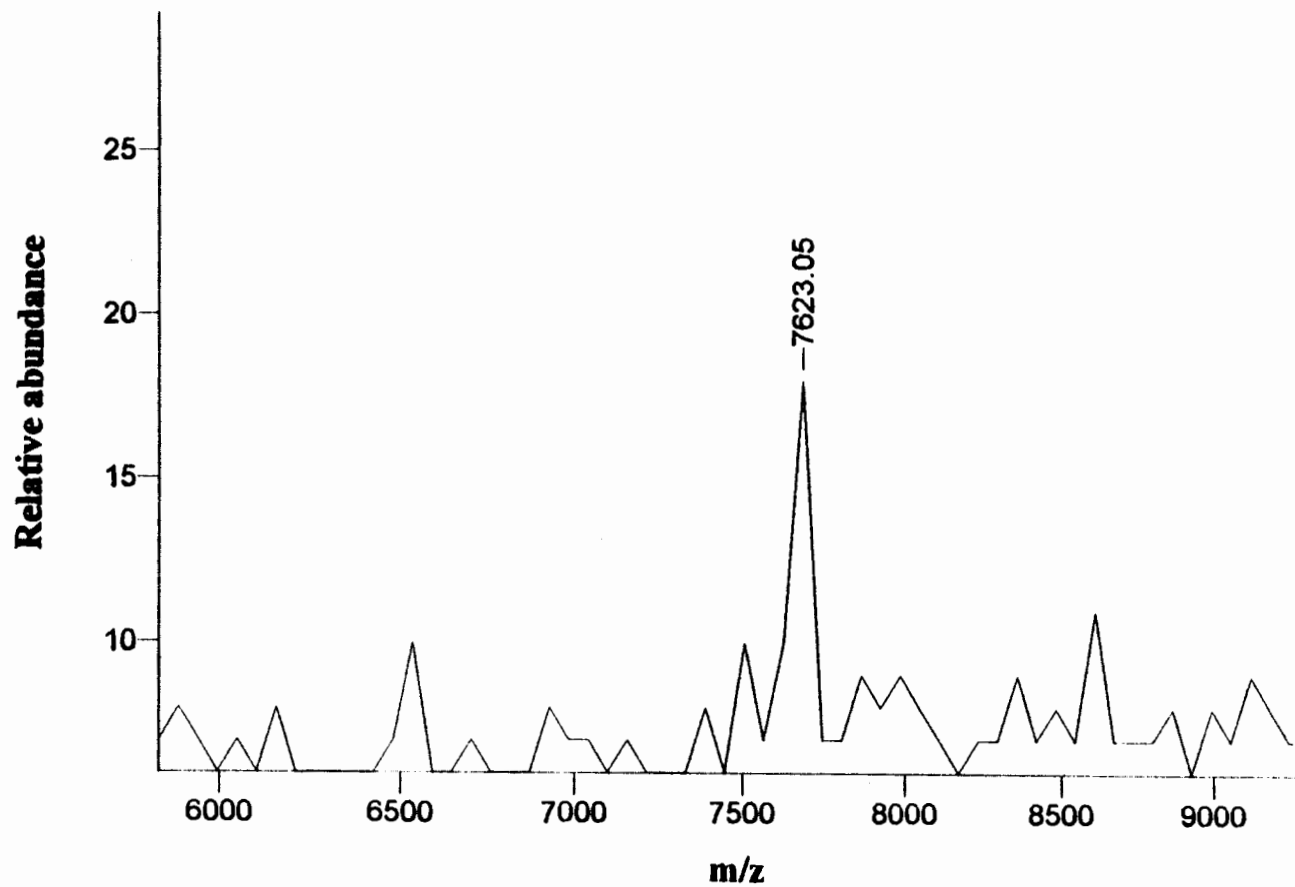


Fig. 29 MALDI MS spectrum of tryptic digest of α 99XLHb CNBr fragment

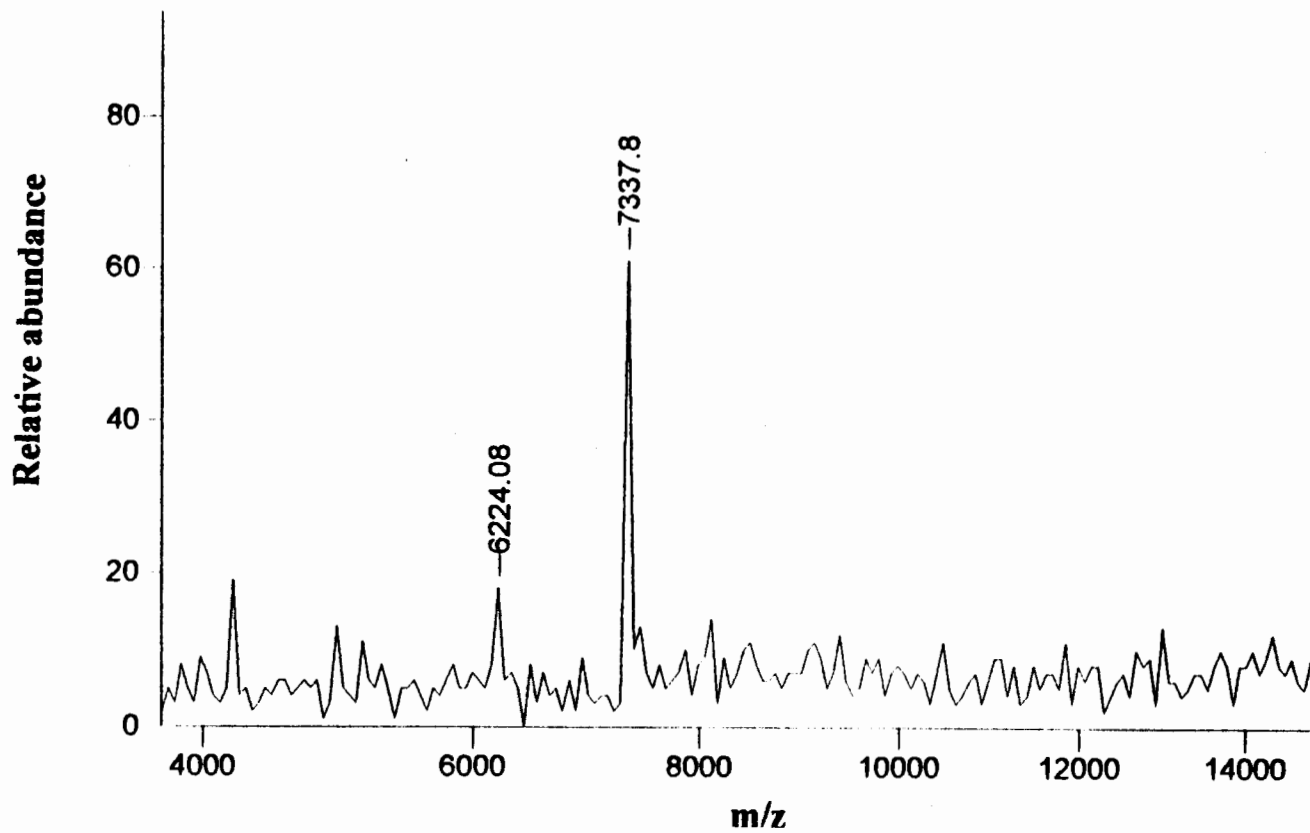


Fig. 30 MALDI MS spectrum of tryptic digest of β 82XLHb CNBr fragment

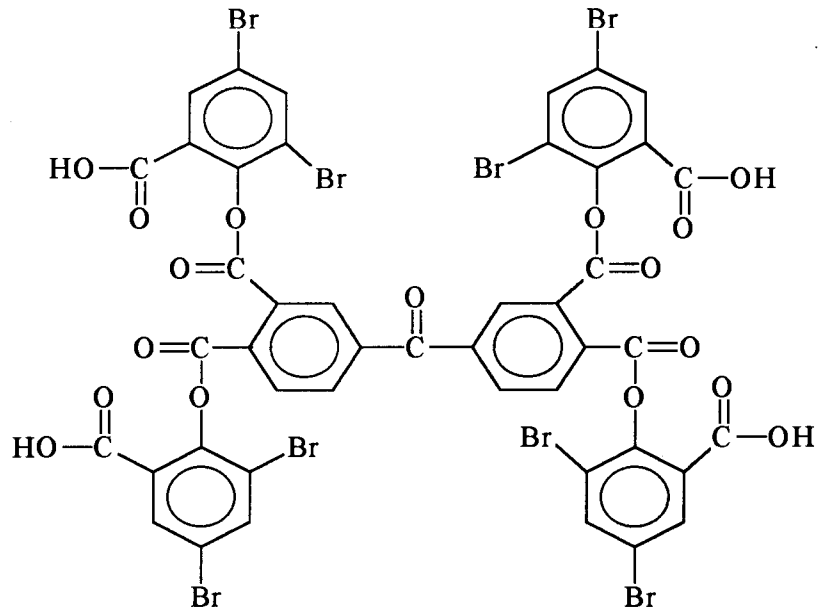
7336.2. These results indicate the method was successful in identifying the sites of the cross-linked hemoglobin.

In summarization, we confirmed the positions of cross-linked site for β 82 XLHb and α 99XLHb. The mass mapping for identifying cross-linked hemoglobin binding site may be applied to the analysis of an unknown cross-linked hemoglobin site.

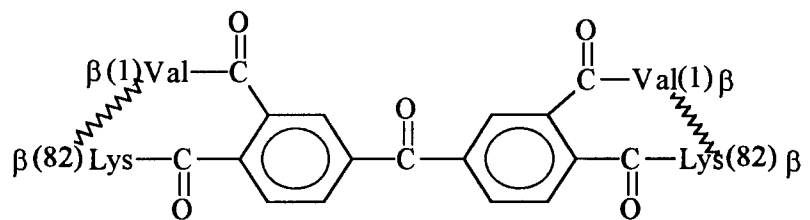
3. Identifying unknown cross-linked hemoglobin

3,3',4,4'-Benzophenone tetra(3,5-dibromosalicylate) (BPTA) is a cross-linking reagent synthesized by Dr. Olsen's group. There were four possible cross-linked sites in the reagent. Once this reagent reacted with hemoglobin, it is possible to tetralink the hemoglobin (see scheme 7). The proposed cross-linking sites are located at β chains of internal valine 1 position and lysine 82 position.

In order to find useful information, we did MALDI mass analyses on the CNBr digest of this product. If the cross-linking reaction take places proposed, we expect fragments at m/z 6000.8 and m/z 8906 to be weak or absent, and expect to observe a fragment at m/z 31,903 (linker mass plus the mass of two β chains). Under current instrument condition, it is very difficult for us to observe this fragment.



3,3',4,4'-benzophenone tetra (3,5-dibromosalicylate) (BPTA)



Proposed BPTA tetralinked hemoglobin

Scheme 7 BPTA reagent and possible product

Fig. 31 is a MALDI spectrum of BPTA cross-linked Hb CNBr digest.

Fig. 31 is a MALDI spectrum of BPTA cross-linked Hb CNBr digest. There are four peaks in the spectrum. The fragments at m/z 9806 and m/z at 7032 were not observed, suggesting that these two fragments were cross-linked. A signal at corresponding to m/z 8292 was observed. We are not sure the origin of m/z 8292. Therefore, the only information we get so far is the cross-linking reaction possible take place between both α chain and β chain other than just in β chain.

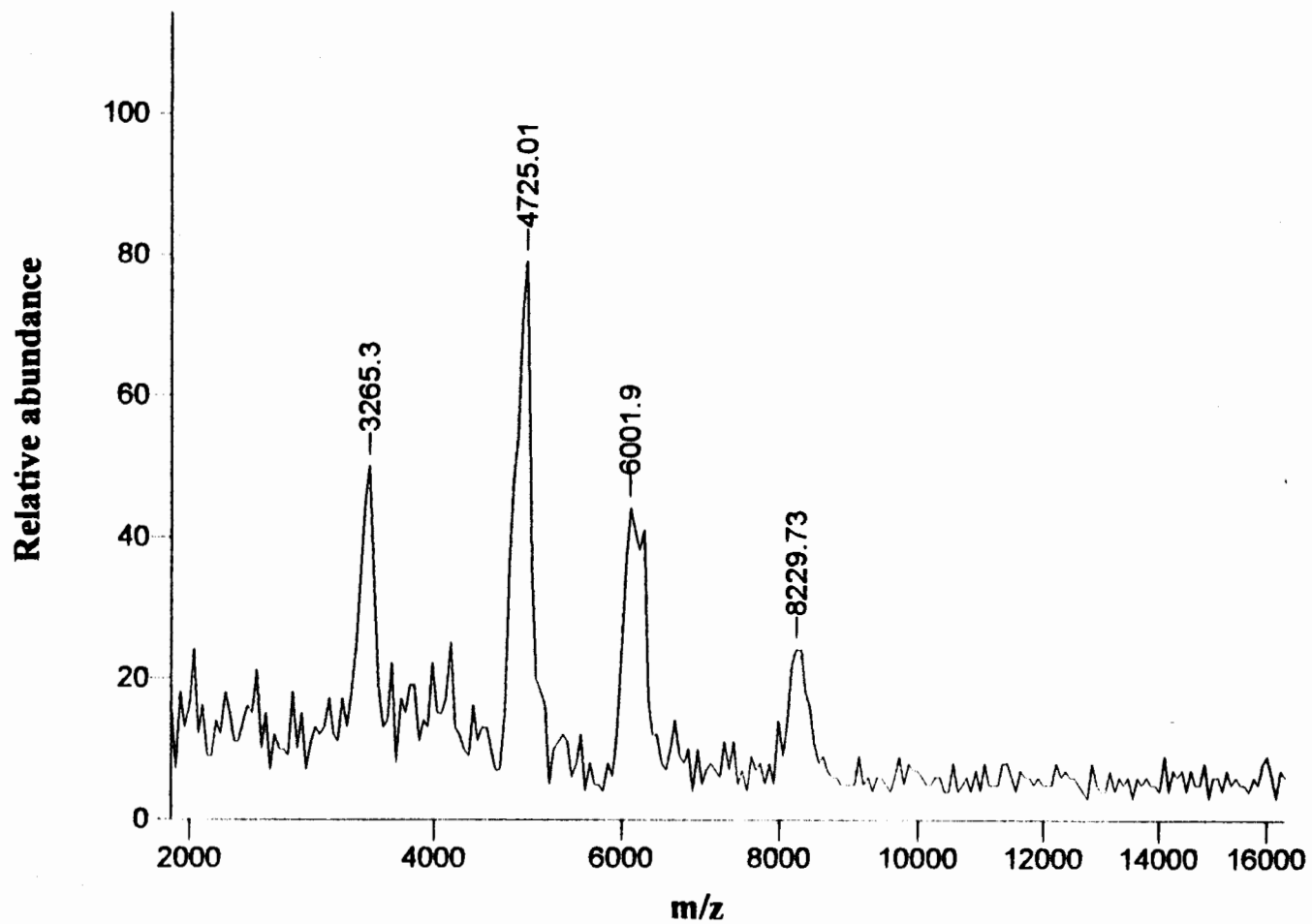


Fig. 31 MALDI MS of CNBr digest of BPTA cross-linked hemoglobin

REFERENCES.

Annan, R. S.; Köchling, H. J.; Hill, J. A.; Biemann, K. *Rapid commun. Mass Spectrom.*, **1992**, 6, 298-302.

Ascoil, F.; Rosaria, M.; Fanelli, R.; and Antonini, E. *Methods in Enzymology*, **1981**, 76, 52-76.

Astle, M. J.; Gergel, C. *J. Org. Chem.*, **1956**, 21 (5), 103-106.

Bahr, U.; Karas, M.; Hillenkamp, F. *Fresenius J. Anal. Chem.*, **1994**, 348, 783-91.

Barber, M.; Bordoli, R. S.; Sedgwick, R. S.; Tyler, A. N. *J. Chem. Soc. Chem. Commun.*, **1981**, 325.

Beckey H. D. in "Principles of field desorption mass spectrometry", **1977**, Pergamon Press, Oxford .

Beavis, R. C.; Chait, B. T. *Rapid Commun. Mass Spectrom.*, **1989**, 4, 436-439.

Beavis, R.C.; Chait, B. T. *Proc. Natl. Acad. Sci., USA*, **1990**, 87, 6873-6877 .

Beavis, R. C.; Chait, B. T. *Anal. Chem.*, 1990, 62, 1836.

Beavis, R. C.; Chait, B. T. *Org. Mass Spectrometry*, 1992, 27, 156-158.

Billeci, T. M.; Stults, J. T. *Anal. Chem.*, 1993, 65, 1709-1716.

Buchanan, M. V.; Hettich, R. L. *Anal. chem.*, 1993, 65, 245A-259A.

Castoro, J. A.; Köster, C.; Wilkins, C. L. *Anal. Chem.*, 1993, 65, 784-788.

Chatterjee, R.; Welty, E. V.; Walder, R.Y.; Pruitt, S. L.; Rogers, P. H. Arnone, A; Walder, J. A. *J. Biol. Chem.*, 1986, 261, 9929-31.

Child, R. G.; Osterberg, A. C.; Sloboda, A. E. ; Tomcufcik, A. S. *J. Pharm. Sci.*, 1977, 66(4), 466-476.

Cody, R. B.; Bjarnason, A.; Weil, D. A., in "Lasers and Mass Spectrometry"

Cotter, R. J. *Anal. Chem.*, 1992, 64,1027A-1039A.

Doroshenko, V. M.; Cotter, R. J. *Anal. Chem.*, 1996, 68, 463-472.

Ehring, H.; Karas, M.; Hillenkamp, F. *Org. Mass Spectrom.*, 1992, 27, 472-480.

Fernandez, E., Ph.D. dissertation, Loyola University Chicago, 1995

George, M.; Wellemans, M. Y.; Cerny, R. L.; Gross, M. L.; Li, K.; Cavalieri, E. L. *J. Am. Soc. Mass Spectrom.*, **1994**, *5*, 1021-1025.

Hames, B. D.; Rickwood, D. in "Gel Electrophoresis of proteins: A Practical Approach", **1990**, 2th ed.; IRK Press: New York.

Hancock, W. S. in "New Methods in Peptide Mapping for The Characterization of Proteins" , **1995**, CRC Press, pp.236.

Henzel, W. J.; Billeci, T. M.; Stults, J. T.; Wong, S. C.; Grimley, C.; Watanabe, C. *Proc. Natl. Acad. Sci. USA*, **1993**, *90*, 5011-5015.

Hill, J. A.; Annan, R. S.; Biemann, K. *Rapid Commun. Mass Spectrom.*, **1991**, *5* 395-399.

Hillenkamp, F.; Unsold, E.; Kautmann, R.; Nitsche, R. *Appl. Phys.*, **1975**, *8*, 341-348.

Huberty, M. C.; Vath, J. E.; Yu, W.; Martin, S. A. *Anal. Chem.*, **1993**, *65*, 2791-2800.

Hutchens, T. W.; Yip, T. T. *Rapid Commun. Mass Spectrom.*, **1993**, *7*, 576-580 .

James, P; Quadroni, M.; Carafoli, E.; Gonnet, G. *Biochem. Biophys. Res. commun.*, **1993**, *195*, 58-64.

Jones, R. T. *Method in Enzymology*, 1994, 231, 321-343 .

Jonscher, K.; Currie, G.; McCormack, A. L.; Yates, J. R., III, *Rapid Commun. Mass Spectrom.*, 1993, 7, 20-26.

Juhasz, P.; Costello, C. E.; and Biemann, K. *J. Am. Soc. Mass Spectrom.*, 1993, 4, 399-409.

Juhasz, P.; Papayannopoulos, I. A.; Zeng, Ch.; Papov, V.; Biemann, K. *Proceedings of the 40th ASMS Conference on Mass Spectrometry and Allied Topics*, Washington, DC, May 31-June 5, 1992, 1913-1914.

Karas, M.; Bachmann, D.; Bahr, U.; Hillenkamp, F. *Int. J. Mass Spectrom. Ion Processes*, 1987, 78, 53-68 .

Karas, M.; Hillenkamp, F. *Anal. chem.*, 1988, 60, 2299.

Karas, M.; Bahr, U.; Giessman, U. *Mass Spectrom Rev.*, 1991, 10, 335-357.

Kebarle, P.; Tang, L. *Anal. Chem.*, 1993, 65(22), 972-986 .

Kluger, R.; Song, Y.; Wodzinska, J.; Head, C.; Fujita, T. S.; Jones, R. T. *J. Am. Chem. Soc.*, 1992, 114, 9275-9279 .

Lee, H.; Lubman. D. M., *Anal. Chem.*, 1995, 67, 1400-1408.

Liao, P. C.; Leykam, J.; Andrews, P. C.; Gage, D. A.; Allison, J., *Anal. Biochem.*, **1994**, 219, 9-20.

Loo, J. A.; Udsoth, H. R.; Smith, R.D. *Anal. Chem.*, **1989**, 179, 404-412 .

Macfarlane, R. D.; Torgerson, F. D. *Science*, **1976**, 109, 920.

Mann, M.; Shen, S.; Fenn, J. B. in "Mass Spectrometry in the Biological Sciences", **1992**, Gross, M. L. Ed., Kluwer Academic Publishers, Dordrecht, pp 145-163 .

Matsudaira, P. in "A Practical Guide to Protein and Peptide Purification for Microsequencing" Second Edit. **1993**, Academic Press, Inc. pp54-59.

Mchugh, J. A. in "Methods of Surface Analysis", A Czanderna, Ed., **1975**, Elsevier, New York .

Meng, C. K.; Mann, M.; Fenn, J. B. *Zeitschr. f. Physik*, **1988**, 10, 361-368 .

Mock, K. K.; Sutton, C. W.; Cottrell, J. S. *Rapid commun. Mass Spectrom.*, **1992**, 6, 233-238 .

Nelson, R. W.; Vestal, M. L. *Proc. 39th ASMS Conf. on Mass Spectrometry and Allied Topics*, **1991**, 332-333.

Posthumus, M. A.; Kistemaker, P. G.; Meuzelaar, H. L. C.; deBrauw, M. C. *Anal. Chem.*, **1978**, *50*, 985.

Robert, E. S.; Hopkins, N. E.; Zaluzec, E. J.; Gage, D. A.; Alworth, W. L.; Hollenberg, P. F. *Biochemistry*, **1994**, 3766-3771.

Schroeder, W. A. in "CRC Handbook of HPLC for the Separation of Amino Acid, Peptides, and Proteins", **1984**, (Hancock, W, S, Ed.) Vol. II, pp. 287-300.

Siuzdak, G. *Proc. Natl. Acad. Sci. USA*, **1994**, *91*, 11290-11297.

Spengler, B.; Kirsch, D.; Kaufmann, R. *Rapid Commun. Mass Spectrom.*, **1991**, *5*, 198-202.

Smith, R. D.; Loo, R. R. O.; Busman, M.; Whitehouse, C. M. *Mass Spectrom. Rev.*, **1991**, *10*, 359-451.

Strupat, K.; Karas, M.; Hillenkamp, F. *Int. J. Mass Spectrom. Ion Process*, **1992**, *27*, 472-480.

Talbo, G.; Roepstorff, P. *Rapid commun. Mass Spectrom.*, **1993**, *7*, 201-204.

Tanaka, K.; Waki, H.; Ido, Y.; Akita, S.; Yoshida, Y.; and Yoshida, T. *Rapid commun. Mass Spectrom.* **1988**, *2*, 151 .

- Vastola, F. J.; Mumma, R. O.; Pirone, A. J. *J Org. Mass Spectrom.*, **1970**, *3*, 101.
- Vestling, M. M.; Murphy, C.M.; Fenselau, C. C. *Anal. Chem.*, **1990**, *62*, 2391-2394.
- Vestling, M. M. *Journal of Chemical Education*, **1991**, *68*(11), 958-960.
- Vorm, O.; Roepstorff, P.; Mann, M. *Anal. Chem.*, **1994**, *66*, 3281-3287.
- Walder, J. A.; Walder, R. Y.; Arnone, A. *J. Mol. Biol.*, **1980**, *141*, 195-216.
- Winslow, R. M. in "Hemoglobin-based red cell substitutes", **1992**, John Hopkins University Press, Baltimore.
- Wu, K. J.; Steding, A.; Becker, C. H. *Rapid Commun. Mass Spectrom.*, **1993**, *7*, 142-146.
- Yates, J. R.; Speicher, S.; Griffin, P. R.; Hunkapiller, T. *Anal. Biochem.*, **1993**, *214*, 397-408.
- Yip, T-T.; Hutchens, T. W. *FEBS Lett.*, **1992**, *308*, 149-153 .
- Zaluzec, E. J.; Gage, D, A.; Watson, J. T. *Protein Expr. and Purif.*, **1995**, *6*, 109-123.

VITA

Xiaomei Gu was born in Wuhan, China.

In August 1981, she entered Jilin University at Changchun, China. She received her degree of Bachelor of Science with a major in chemistry in July, 1985. Then she started work as an instructor in the Department of Chemistry at Guizhuo University.

In September, 1987, She entered Research Center for Eco-Environmental Sciences, Academia Sinica. She received her degree of Master of Science with a major in environmental Chemistry in August 1990. Then She worked there as a research Scientist from 1990 to 1991.

In September 1993, she enrolled in the Chemistry Department at Loyola University of Chicago as a part time student. In September 1994, she received assistantship and became a full time student. She is currently completing the degree of Master of Science at Loyola University of Chicago in 1996.

THESIS APPROVAL SHEET

The thesis submitted by Xiaomei Gu has been read and approved by the following committee:

M. Paul Chiarelli, Ph. D., Director
Assistant Professor, Chemistry
Loyola University Chicago

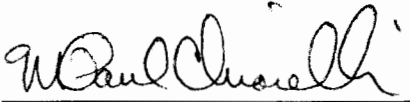
Alanah Fitch, Ph. D.
Professor, Chemistry
Loyola University Chicago

Kenneth W. Olsen
Professor, Chemistry
Loyola University Chicago

The final copies have been examined by the director of the Committee and the signature which appears below verifies the fact that any necessary changes have been incorporated and that the thesis is now given final approval by the committee with reference to the content and form.

The thesis is, therefore, accepted in partial fulfillment of the requirements for the degree of Master of Science.

8/27/96
Date


Director's signature